Laney

Thermal effects in air cooled turbine blades.

THERMAL EFFECTS IN AIR COOLED TURBINE BLADES

Submitted to the Graduate Faculty

of the

University of Minnesota

by

J. S. Laney

Lt USN

In Partial Fulfillment of the Requirements

for the

Degree of Master of Science

in

Aeronautical Engineering

May 1952

TABLE OF CONTENTS

SUMMARY

To date, it has not been clearly indicated how varying the area and perimeter over the span of an air cooled turbine blade will affect the spanwise blade temperature distribution. It is therefore the purpose of this experiment to make such an investigation. The effect on the inside film heat transfer coefficient will also be investigated.

Three test blades were used, one with constant area and perimeter over the blade span, and two with variously tapered internal fins. Tests were made at gas temperatures of 800°F and 1100°F. Maximum cooling air flow, Wa, was, Wa = .925 lbs/min. Exclusive of the leading and trailing edges of the blades, the cooling air was so arranged as to give a uniform temperature over the chord of the main body of the blade. This was true at all spanwise stations.

The following conclusions were reached:

1. Varying the area and perimeter over the blade span did not affect the spanwise blade temperature distribution at zero cooling air flow. As the cooling flow was increased, the spanwise blade temperature distribution from root to middle span for all test blades was essentially the same. From middle span to tip, the blades with less cooling surface showed a noticeable decrease in blade temperature reduction.

2. The ratio of inside to outside film heat transfer coefficient remained essentially independent of gas temperature as well as changes in area and perimeter over the blade span.

3. Over the range tested, the ratio of inside to outside film heat transfer coefficient increased linearally with the cooling air flow.

This investigation was conducted in the Gas Turbine Test Cell of the Main Engines Laboratory of the Mechanical Engineering Department at the University of Minnesota, Minneapolis, Minnesota.

INTRODUCTION

Maximum effort in the development of gas turbines is being exerted to improve specific power output, to reduce specific fuel consumption and to increase reliability. The most promising field for the attainment of these objectives lies in increasing the turbine inlet temperature. At present uncooled gas-turbine-engine performance is limited because the temperature at the turbine inlet cannot exceed about 2000°R, however existing hydrocarbon fuels can produce far higher temperatures, approximately 4000°R.

An immediate means for solution of the foregoing problem is turbine blade cooling. From a theoretical analysis of the various methods of cooling turbine blades, Ref. 1, it has been found that sufficient improvements in the efficiency of gas turbine engines may be obtained through cooling the turbine blades to justify extensive research in turbine cooling.

Boundary layer control, cooling the rim of the rotor, and cooling hollow blades internally with air or liquid offer possibilities of substantial increases in permissible gas temperatures. Cooling of the tip of the blade and coating the blade with ceramic have been relatively ineffective, Ref. 1. NACA scientists have expressed great faith however in the future of ceramel, a combination of ceramics and metals, as a blade material replacing present strategic materials, Ref. 2.

A comparison of the relative effectiveness of different methods of cooling show theoretically that the multiple fin air cooled blade provides a solution to the double objective to be obtained by operation at higher gas temperatures and use of non strategic materials, Ref. 3. In this connection NACA has suggested that packing the blade cooling cavity with small metal tubes brazed in place would be a practical production method of getting equivalent increase in cooling area without complications of mass-producing internal blade fins, Ref. 2.

To date, investigators in making theoretical analysis of spanwise temperature distribution in various types of air cooled blades have made the basic assumption that the variations in area and perimeter are negligable over the blade span, Ref. 3. It has been pointed out by these same investigators that this assumption can be eliminated only if numerical solutions are determined. Calculations reveal that when the above factors are allowed to vary and numerical solutions are used, very little difference in the spanwise blade-temperature distribution results. However the same investigators stated that the blade temperature distribution is sensitive to selection of the average inside heat transfer coefficient which in turn is dependent upon the passage configuration, Ref. 3. Therefore the question as to how tapering the internal fins in a turbine blade will effect

spanwise blade temperature distribution and inside heat transfer coefficient is not adequately answered in the theoretical analysis.

Internally finned air cooled blading appears to offer greater possibilities for future use as compared to other blade configurations and methods of cooling. Tapering of turbine blades to reduce high centrifugal stresses is of importance also. Therefore it is the purpose of this experiment to investigate how variously tapering the fins will affect the spanwise blade temperature distribution and inside film heat transfer coefficient.

This investigation was conducted in March 1952 by LT J. S. Laney USN in the Main Engines Laboratory of the Mechanical Engineering Department at the University of Minnesota, Minneapolis, Minnesota. The author would like to express his appreciation to Dr. E. R. G. Eckert and Dr. N. A. Hall of the Department of Mechanical Engineering for their advice and suggestions in the prosecution of this investigation.

TEST EQUIPMENT

The three test blades used are in fact three test bodies that could be fabricated with some degree of facility. They were also made large enough to imbed thermocouples to the desired spanwise depth in the blade skin. Fig. 1 is a two view drawing showing the root end and plan view of all blades. Fig. 2 shows the side view of each blade and indicates the manner in which the fins were tapered. Fig. 3 and Fig. 4 are photographs of the three test blades showing the root ends and tip ends with thermocouples imbeded. The blade body consists of two half sections milled from mild steel. The leading as well as trailing edge were made from two, 1/8 inch, mild steel sections and a 3/16 inch mild steel rod, all welded into a "V" section. This assembly was then welded on to the two main half sections. There are twenty fins in each blade, .1 inch wide and spaced .05 inches apart. The blade chord is 4.3 inches and blade span in the test section is 4.5 inches.

A total of eleven, 1/8 inch holes were drilled in the blade skin from root and tip end to three different spanwise levels in the blade. Fig. 5 shows the manner in which the holes were drilled and the thermocouples located. The thermocouples were made with 30 B&S gage glass insulation, iron-constantan

thermocouple wire. They were read on a Leeds and Northrop Potentiometer Indicator having a scale from 0-2000°F. Beaded junctions were made by the arc method as outlined in Ref. 4. Two hole porcelain insulators ground to 1/8 inch size were used to insulate the wire inside the blade hole. The insulated thermocouples were imbeded in the blade itself with Sauereisen Porcelain Cement Number 29.

Each blade was fitted with a flange at the root end for securing to the top of the test section. The tip end of the blade fitted into an adapter plate in the bottom of the test section and was sealed with Sauereisen High Temperature Cement Number 1 to prevent any hot gas leaks. A cooling air entrance manifold 4 inches high and the same width and length as the test blade root was fitted over the root end of the blade with a matching flange. Cooling air entered the manifold through 3/8 inch taps located at both ends of the manifold 1/2 inch from the top. The wires from the thermocouples were lead out two 1/8 inch taps in the top of the manifold. These holes were also sealed with Sauereisen High Temperature Cement Number 1 to prevent any cooling air leaks. An exit cooling air manifold was fitted over the tip end of the blade on the bottom of the test section. A 3/8 inch tap in the bottom of this manifold allowed the cooling air to escape over the beaded junction of a thermocouple cemented on the outside surface of the manifold.

Thermocouple wires were lead out in the same manner as for the cooling air entrance manifold.

The test section was made from 1/8 inch mild steel and was 18 inches long, 4.5 inches high and 3.5 inches wide. All blades were located 9 inches downstream from the entrance to the test section. Gas temperature at various levels in the test section was measured 6 inches upstream of the test blade. The temperature probe used, consisted of a 3/16 inch steel tube in which an insulated thermocouple was imbeded in Sauereisen Porcelain Cement Number 29. A radiation shield made of 3/8 inch copper-nickel tubing 1 1/8 inch long was placed at the end of the probe to shield the beaded junction. Three static pressure taps were employed 2 1/2 inches upstream of the blade to measure test section static pressure. One tap was located on the top of the test section, and the other two taps on the side. A total pressure tube was also located 2 1/2 inches upstream of the blade to measure test section total pressure. All specifications for pressure measurements were complied with as outlined in Ref. 5.

Fig. 6 is a photograph of the interior of the test cell and shows the test section and over all test setup. A Lycoming Model O-435-T air cooled engine, rated at 162 HP at 2800 RPM, drove directly a 7.48:1 gear ratio centrifugal compressor from an Allison V-1710 aircraft engine. The air which was delivered by the compressor to a large manifold was ducted to the single combustion chamber of an Allison J 33-A-17 turbojet engine. The exhaust of this burner was connected directly to the test section.

A spark ignited acetylene flame was used to start the burner diesel fuel spray.

Air flow to the burner was measured by an orifice 5.6 inches in diameter. This orifice was placed in an 8 inch duct on the intake side of the engine driven compressor. Pressure differential across the orifice was measured by a water manometer at the control panel. A thermocouple at the duct inlet measured burner air inlet temperature.

Number 1 Energee diesel fuel was supplied to the burner by an electrically driven aircraft fuel pump. Weight flow was measured by a type 5A-60 fuel flowrator placed in the line.

A compressed air line in the test cell supplied cooling air for the blade, and the rate of flow was measured by a type 5A-25 Fischer and Porter flowrator. A pressure gage and thermocouple were placed in the line to obtain data for converting readings to weight flow.

The control panel outside the test cell contained all engine and burner controls as well as engine instruments, pressure gages, temperature selector switch, potentiometer indicator, and manometers. Fig. 7 is a photograph of the control panel.

TEST PROCEDURE

Prior to starting the jet burner, the engine and compressor were warmed until oil temperatures read above 120°F. At about 1000 engine RPM the electric spark was first turned on and then the acetylene jet was cut in. When the test section temperature as indicated by the temperature probe registered a decided increase, the fuel was cut in. A further rise in temperature indicated the fuel had been ignited. Fuel pressure was then built up by the fuel control, and engine RPM increased simultaneously until 2500 RPM and the desired gas temperature was reached. The acetylene and spark were shut off at about 600°F. All runs were made at 2500 RPM and only the fuel control was utilized to control the test section gas temperature. Cleaning the fuel nozzle in the burner after each run enabled the operator to obtain very fine control over the gas temperature by controlling the fuel flow.

At gas temperatures of 800°F and 1100°F as measured by the gas temperature probe in the middle of the test section, the cooling air flow was varied and all instruments were read. Table I is a compilation of these readings for all three blades. Great care was exercised in making sure equilibrium conditions existed when readings were made. A plot of several blade temperatures versus time was kept, and when successive temperatures

indicated no change, readings were taken. Readings leveled off in approximately three minutes, but a wait of five minutes was always registered.

Prior to commencing test runs, all permanently installed leads in the test cell leading into the control panel were disconnected and blown free of water and other foreign material. The cooling air flow flowrator was also calibrated in accordance with Ref. 6. Prior to each run all connections and leads were tested for leaks. Because of the inaccessiblity of the inside of the test section, it was impossible to check for leaks in connections at the test section.

ANALYSIS OF RESULTS

A compilation of all test data can be found in Table I. Table II is a compilation of all reduced data. Results are shown graphically in Fig's. 8 to 21.

A probe of the gas temperature in the test section at 800°F reference temperature, the temperature in the middle of the test section, revealed that the gas temperature of the test section 1/4 of the distance down from the top was about 20° less than 800°F. The gas temperature 3/4 of the distance down from the top and corresponding to the 3/4 span level was greater than 800°F by about 20°. Therefore it was felt that the temperature in the middle of the test section could be taken as the average value for the test section gas temperature. This difference in gas temperature in the test section could be attributed to uneven combustion or the manner in which the hot gases were ducted from the combustion chamber to the test section. Also the fact that more heat would be dissipated from the top of the test section than the bottom would account for part of it. An estimate of the amount of error to be expected in gas temperature measurement due to conduction losses in the probe revealed that as long as the probe remained over 3/4 inches from the test section wall the error would be within the allowable of ± 8°F, calculation No. 1(a). It was found that as the probe approached

the wall the conduction losses became quite great. An estimate of the radiation loss from the beaded junction of the gas temperature probe thermocouple to the test section walls, and the radiation gain from the combustion flame to the bead showed the net effect to be negligable, calculation No. 1(b). Never-theless a radiation shield was installed on the probe to guard against any undue radiation effects.

An effort was made in this investigation to obtain enough temperature readings, both spanwise and chordwise in the blade, to indicate trends and to serve as checks. For this reason chordwise temperatures at each spanwise station were taken on both sides of the blade, Fig. 5. Three spanwise levels were chosen at 1/4 span, 1/2 span and 3/4 span. Each spanwise station had three temperatures and were located at approximately 1/4 chord, 1/2 chord and approximately 3/4 chord. This arrangement gave three separate determinations of spanwise temperature distribution in the main body of the blade. The leading and trailing edge temperatures were only determined at the 1/2 span level. The gas temperature used as the reference temperature was obtained at this same level also, even though a probe of the test section was made at each run.

From the very nature of the design of the blade a complicated cooling system would have had to have been devised to maintain a uniform temperature over the entire chord of the blade. Therefore for reproducibility of results, since the leading and trailing edge temperatures were not deemed particu-

larly important in this investigation, the cooling air was arranged to give a constant temperature over the chord of the main body of the blade. Considering the probable error, calculation No. 2, Fig's. 8 to 13 show that this was essentially obtained at all spanwise levels for all cooling air flow rates. Fig's. 8 to 13 show the chordwise blade temperature distribution at the various spanwise levels at various cooling air flow rates.

All blades at zero cooling air flow show similar trends. The 1/2 spanwise level has the highest temperature, the 3/4 span level is next and the 1/4 span has the coolest temperatures. This is as might be predicted. The flow of heat is from the middle to the outside ends of the blade where there are cooler surroundings and where more heat may be conducted away. In each instance the chordwise temperature distribution of all blades at a given gas temperature and spanwise level is the same.

There are two reasons why the leading and trailing edge temperatures of all blades at zero cooling flow are higher than the main body temperatures. Part is caused by the fact that there are no cooling fins near the leading and trailing edge of the blade. Therefore less heat is conducted away from them. Another factor is the dynamic temperature increase at the leading edge, Ref. 7. When the velocity is diminished to zero, such as at the leading edge, the kinetic energy is transformed into

heat. In the boundary layer on the surface of the blade the velocity of the gases is diminished by frictional forces and its kinetic energy is also transformed into heat. However not as much of the kinetic energy is so transformed. Only a certain amount of the kinetic energy is recovered as against 100 percent recovery for a stagnation point. This recovery factor is dependent on the type of surface and the nature of the flow. The over all temperature increase, θ, of the leading edge of the three test blades over the body of the blades was calculated to be, $\theta = 5.67°F$ for a gas temperature of 800°F, and $\theta = 6.96°F$ for a gas temperature of 1100°F, calculation No. 12.

Examination of Fig's. 8 to 13 further show for each blade a uniform pattern of chordwise temperature distribution at various cooling air flows. In every case the 1/4 span level is cooled the greatest, the 1/2 span level is next and the 3/4 span level is cooled the least. There is very little difference between the three blades in the chordwise temperature distribution at the 1/4 spanwise level. At the 1/2 span level, blades 2 and 3 with less cooling area start to show a decrease in blade temperature reduction and at the 3/4 span level blades 2 and 3 have shown a very noticeable decrease in blade temperature reduction. This is as might be predicted also, since with more cooling surface more heat should be dissipated.

Fig's. 14 to 16 show the blade temperature reduction spanwise in the blade at the three different chordwise locations

mentioned previously. Again it can be seen that the blade temperature reduction at the 1/4 span level is essentially the same in all three blades. However as the tip is approached, the blades with reduced fin area, therefore less cooling area, show less and less blade temperature reduction. All three spanwise blade temperature gradients in each blade are practically identical and show that cooling conditions and blade temperature distribution throughout the main body of each blade were uniform.

From Fig's. 14 to 16 it can be noticed that there was a greater blade temperature reduction at the higher gas temperatures. However a determination of the ratio of blade temperature reduction to gas temperature less cooling air entrance temperature, ϕ , reveals that the heat transfer coefficient, h, and the thermal conductivities, k, are essentially the same for all gas temperatures, Fig's. 17 to 19. This agrees with both the heat transfer theory and the findings of other investigators, Ref. 7. Considering the calculated probable error, the values for ϕ at 800°F and 1100°F show very close agreement. Again a check of all three spanwise gradients in each blade show practically identical results.

From the data obtained, a determination of the ratio of inside to outside film heat transfer coefficient was made by making a heat balance between the outside and inside of the

blade, calculation No. 8. In this equation a fin effectiveness factor was introduced, Ref. 8 and Ref. 7. This fin effectiveness factor is a ratio of the heat actually dissipated by the fin to the heat that would be dissipated if the surface of the fin was at the same temperature as the base of the fin. This factor is necessary since the inside wall temperature was used for the heat balance and not the temperature of the fin. Fin effectiveness for all three blades was found to be very nearly equal to one, calculation No. 7.

Since the middle blade wall temperatures only were recorded, it was necessary to make an estimate of the change in temperature across the blade wall so that the inside and outside wall temperatures could be determined for the heat balance equation.

It was determined that the flow inside the blade was laminar from a Reynold's Number calculation of the maximum cooling air flow through the blades, calculation No. 3.

For an estimate of the inside heat transfer coefficient an expression involving a constant Nusselt's Number was utilized, Ref. 7, calculation No. 4. This expression was for fully developed flow in the cooling air passage. Another expression which involved a variable Nusselt's Number and which applied for a flat plate boundary layer was also considered. However from

calculations of the heat transfer coefficient using both equations it was determined that fully developed flow was being obtained.

An estimate of the outside heat transfer coefficient was determined for flow of gases parallel to plane surfaces, Ref. 9, calculation No. 5. With these two estimated heat transfer coefficients for the outside and inside of the blade, the blade temperature difference, ΔT, was determined in accordance with Ref. 7, calculation No. 6, and found to be, ΔT = 2.02°F for gas temperature 800°F, and ΔT = 3.66°F for a gas temperature of 1100°F.

Fig. 20 is a plot of the ratio of inside to outside film heat transfer coefficient as finally determined by the heat balance equation, calculation No. 8. It is noted that the ratio is essentially independent of gas temperature and blade configuration, therefore changes in perimeter or area over the blade span. It might be predicted that the inside film heat transfer coefficient would be the same for blade 1 and 2. Blade 1 has no taper, and blade 2 has taper by reducing fin height at the tip. This would cause the cooling air flow to accelerate. However since the flow inside the blades has been determined to be laminar, the heat transfer coefficient would be independent of this change in velocity. Blade 3 which has an expanding air

cooling passage with reduced fin area presents somewhat different conditions. Here the flow might be predicted to separate and the heat transfer coefficient change.

As the cooling air flow is increased, the ratio of inside to outside film heat transfer coefficient increases. Fig. 21, which is a cross plot of Fig. 20, reveals that over the range investigated, the ratio of inside to outside heat transfer coefficient increases linearally with the cooling air flow.

All calculations of the ratio of inside to outside film heat transfer coefficient were made for the 1/2 spanwise level. All blade dimensions and temperatures used were recorded for this same level also.

From Fig. 20 it can be seen that at the highest cooling air flow, blade 2 is shown to diverge from the average heat transfer coefficient ratio value as determined for the other blades. Since it fell in line at the lower cooling air flows, the only conclusion is that these are bad points and should be disregarded. This is most likely caused by the fact more cooling air flow than was recorded was passing through the blades.

CONCLUSIONS

The following conclusions have been drawn from the results obtained from varying the area and perimeter over the span of air cooled turbine blades.

1. Varying the area and perimeter over the blade span did not effect the spanwise blade temperature distribution at zero cooling air flow. As the cooling air flow was increased, the spanwise blade temperature distribution from root to middle span for the three test blades remained essentially the same, but from middle span to tip, the blades with less cooling surface, therefore reduced fin area, showed a noticeable decrease in blade temperature reduction. Blade 1 with straight fins proved to be the best blade from a cooling stand point.

2. The ratio of inside to outside film heat transfer coefficient remained essentially independent of gas temperature and changes in area and perimeter over the blade span.

3. Over the range tested, the ratio of inside to outside film heat transfer coefficient increased linearally with the cooling air flow.

REFERENCES

1. Sanders, J. C. and Mendelson, Alexander; "Theoretical Evaluation of Methods of Cooling the Blades of Gas Turbines"; NACA RM E7B11g, April 1947.

2. McSurely, A.; "NACA Shows Cooler Blades for Hot Jets"; Aviation Week, October 22, 1951.

3. Livingwood, John N. B. and Brown, W. Byron: "Analysis of Spanwise Temperature Distribution in Three Types of Air Cooled Turbine Blades"; NACA TR 994, March 1951.

4. Baker, H. Dean; "Manual on Thermometry with Emphasis on Thermocouple Techniques"; 1950, Pratt and Whitney Aircraft Division of United Aircraft Corporation, East Hartford, Conn..

5. "Pressure Measurements"; 1940, American Society of Mechanical Engineers, New York.

6. "Flow Measurement"; 1940, American Society of Mechanical Engineers, New York.

7. Eckert, E. R. G.; "Introduction to the Transfer of Heat and Mass"; 1950, 1st ed., McGraw-Hill Book Company, Inc., New York.

8. Jacob, Max; "Heat Transfer Volume I"; John Wiley and Sons, Inc., New York.

9. Brown, A. I. and Marco, J. M.; "Introduction to Heat Transfer"; 1942, 1st ed., McGraw-Hill Book Company, Inc., New York.

10. Jennings, J. C.; "Air Cooling of a Horizontally Grooved Turbine Blade Model with Covering Metal Sleeve"; M. S. Thesis, University of Minnesota, 1951.

11. Rasmussen, A. L.; "Air Cooling of a Slotted Gas Turbine Blade"; M. S. Thesis, University of Minnesota, 1951.

12. Pollmann, Erich; "Temperatures and Stresses on Hollow Blades for Gas Turbines"; NACA TM 1183 September 1947.

13. Kohlmann, H.; "The Development of a Hollow Blade for Gas Turbines"; NACA TM 1289, December 1950.

APPENDIX

TABLE I

Data as Recorded For Air Cooled Finned Turbine Blade Models

All Temperatures in Degrees Fahrenheit

Cooling Air Pres at Flow rator	Cooling Air Quantity Flowrator	Test Section Total Pressure	Test Section Static Pressure "Hg gage Take = 2.0			Burner Air Intake Orifice	Burner Fuel Flow Flowrator	Thermocouples in Test Blade										Test Section Total Temperature			Burner Air Inlet Temp.	Cooling Air Inlet Temp.	Cooling Air Exit Temp.
P_A psig	Q_A cfm	P_0 "Hg	P_{S_1}	P_{S_2}	P_{S_3}	h_w "H_2O	W_f lb/hr	T_1 •	T_2 •	T_3 ○	T_4 ○	T_5 •	T_6 •	T_7 ○	T_8 •	T_9 ⌀	T_{10} ⌀	T_{15} ⌀	¼ height ⌀	½ height T_{14} •	¾ height ○	T_{11}	T_{12}	T_{13}
TEST BLADE 1 Straight Fin																							
	0	3.6	1.18	1.3	1.21	19.5	84	775	755	720	718	755	755	740	762	790	745	742	822	800	760	48		
6.7	4	3.6	1.18	1.3	1.21	19.5	84	735	668	618	608	661	668	610	700	670	676	666		800		45	76	307
16.0	6	3.6	1.18	1.3	1.21	19.5	84	720	630	570	557	614	624	563	668	629	630	625		800		50	75	270
23.6	8	3.6	1.18	1.3	1.21	19.5	84	710	604	543	525	582	598	528	642	597	608	589		800		48	75	248
	0	4.45	1.15	1.3	1.18	18.5	114	1053	1020	956	945	1015	1023	958	1030	1010	1015	1013		1100		50		
6.7	4	4.45	1.15	1.3	1.18	18.5	114	998	870	815	805	885	893	811	948	910	920	910		1100		50	75	400
16.0	6	4.45	1.15	1.3	1.18	18.5	114	988	878	763	752	838	850	760	920	865	875	867		1100		48	75	372
22.0	8	4.45	1.15	1.3	1.18	18.5	114	973	805	716	704	785	810	714	888	820	831	825		1100		50	75	338
Barometer 29.22" Hg																							
Ambient Temp. 72 °F																							
TEST BLADE 2 Tapered Fin																							
	0	3.4	.93	1.02	.98	19.3	84	764	750	710	718	745	750	710	752	739	740	740	811	800	779	32		
6.8	4	3.4	.93	1.02	.98	19.3	84	707	678	609	613	675	677	609	692	681	692	692		800		36	71	310
13.5	6	3.4	.93	1.02	.96	19.3	84	682	650	578	583	645	655	578	680	673	675	675		800		38	72	290
25.4	8	3.4	.93	1.02	.96	19.3	84	630	589	510	522	589	602	515	650	625	622	628		800		40	72	242
	0	4.3	.80	.98	.82	18.45	116	1047	1015	949	963	1013	1020	955	1020	1008	1009	1009		1100		40	75	
6.9	4	4.3	.80	.98	.82	18.45	116	960	920	814	835	921	932	830	951	959	960	960		1100		40	75	416
13.7	6	4.3	.80	.98	.82	18.45	116	909	870	760	784	875	890	760	926	925	925	928		1100		40	75	390
25.0	8	4.3	.80	.98	.82	18.45	116	842	785	662	700	790	814	688	870	855	850	860		1100		40	75	315
Barometer 29.02" Hg																							
Ambient Temp 71 °F																							
TEST BLADE 3 Tapered Fin																							
	0	3.3	1.0	1.15	1.08	19.45	89	770	755	717	725	752	758	718	756	749	748	748	820	800	808	42		
7.3	4	3.3	1.0	1.10	1.02	19.25	84	740	695	610	610	685	690	598	710	710	718	708		800		45	75	327
15.8	6	3.3	1.0	1.10	1.02	19.25	84	730	665	574	576	655	662	560	690	690	693	688		800		45	75	270
22.0	8	3.3	1.0	1.10	1.02	19.3	89	718	639	542	542	630	638	530	668	668	674	670		800		45	75	245
	0	4.2	.92	1.1	1.0	18.4	114	1050	1025	955	970	1015	1028	955	1030	1012	1020	1018		1100		45		
7.4	4	4.2	.92	1.1	1.0	18.4	114	1022	955	830	838	939	955	820	977	974	969	978		1100		48	75	435
17.0	6	4.2	.92	1.1	1.0	18.4	114	1008	910	768	776	897	910	755	950	950	951	951		1100		48	75	370
24.0	8	4.2	.85	1.02	.9	18.4	114	990	872	723	736	860	872	716	928	920	930	920		1100		48	75	300
Barometer 29.22 "Hg																							
Ambient Temp 71.5 °F																							

TABLE II

Reduced Data

Test Section Total Temp	Cooling Air Flow Rate uncorrected	Cooling Air Flow Rate Corrected	Weight Flow of Cooling Air 100°F 14.7 psia	Burner Air Flow Rate	Burner Fuel Flow Rate	Test Section Mach Number	Mach Number at Blades	Ratio of Inside to Outside Film Heat Transfer Coefficient of Blades
T_o °F	Q_A cfm	Q_1 cfm	W_A lb/sec	W lb/hr	W_f lb/hr	M_T	M_B	h_i/h_o
Test Blade I Straight Fin								
800	4	4.88	.00578	9620	84	.300	.388	.1062
800	6	8.82	.01043	9620	84	.300	.388	.148
800	8	13.18	.0156	9620	84	.300	.388	.178
1100	4	4.88	.00578	9350	114	.294	.382	.1205
1100	6	8.82	.01043	9350	114	.294	.382	.153
1100	8	12.9	.01528	9350	114	.294	.382	.1895
Test Blade II Tapered Fin								
800	4	4.93	.00584	9620	84	.303	.372	.1218
800	6	8.48	.01004	9620	84	.303	.372	.1535
800	8	13.5	.01597	9620	84	.303	.372	.2275
1100	4	4.92	.00582	9350	116	.300	.369	.124
1100	6	8.50	.01007	9350	116	.300	.369	.165
1100	8	13.4	.01585	9350	116	.300	.369	.242
Test Blade III Tapered Fin								
800	4	4.96	.00587	9620	84	.294	.382	.1192
800	6	8.825	.01043	9620	84	.294	.382	.1515
800	8	12.91	.01528	9620	84	.294	.382	.1635
1100	4	4.98	.00588	9350	114	.294	.382	.1159
1100	6	8.98	.01061	9350	114	.294	.382	.1512
1100	8	13.22	.01565	9350	114	.294	.382	.182

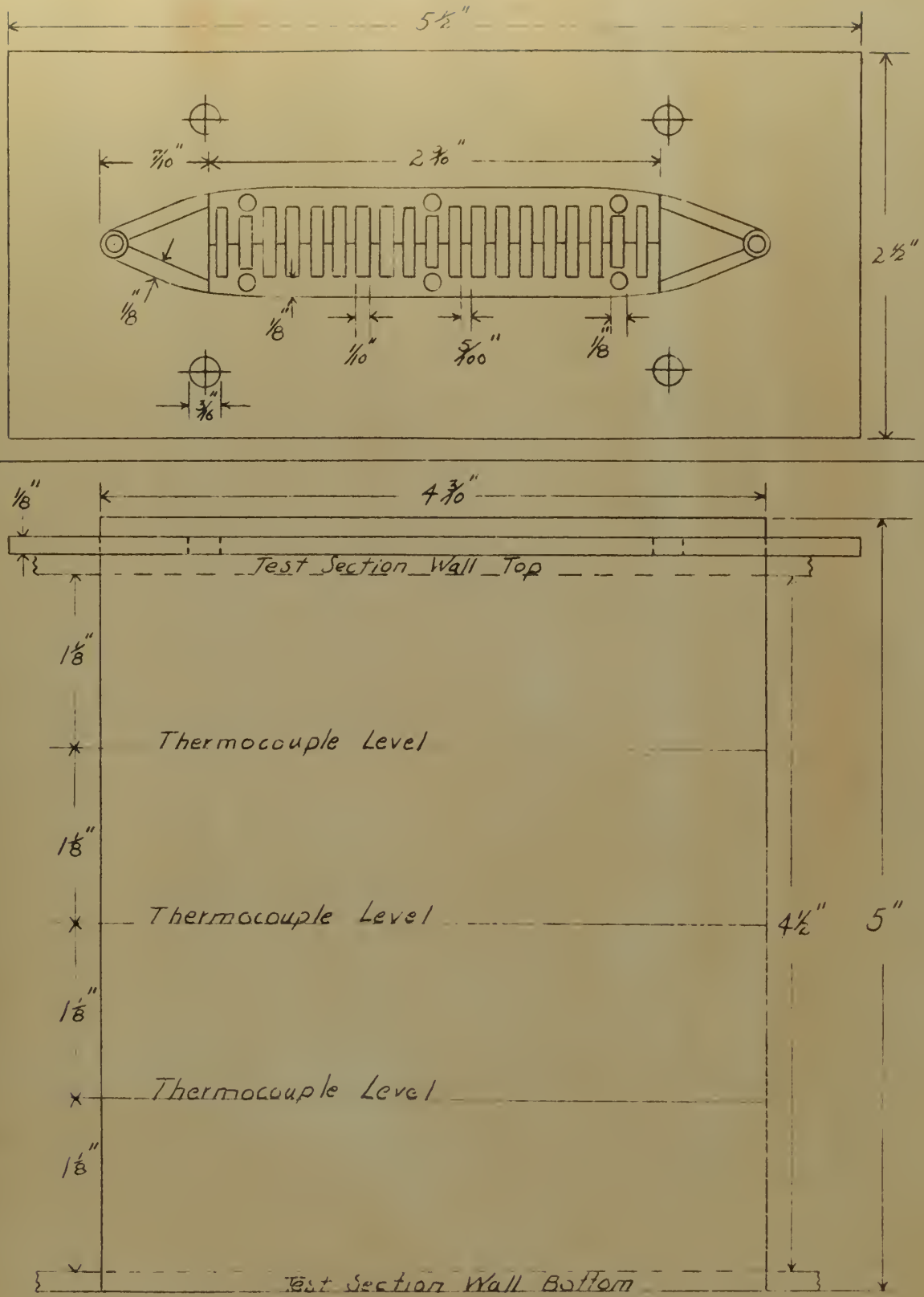

Root End View and Plan View
of All Test Blades Full Scale

Fig. 1

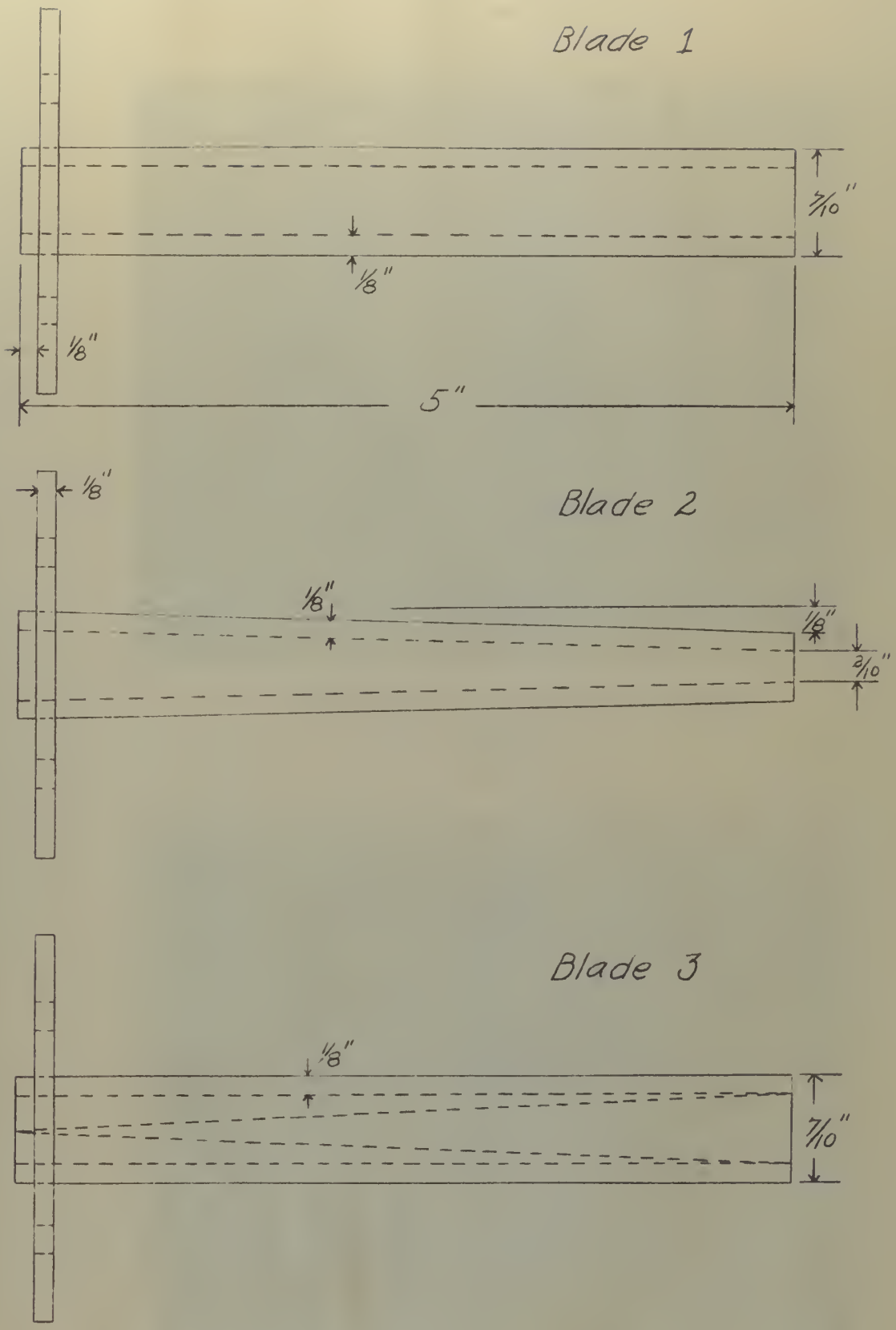

Side View of Test Blades
Showing Fin Configuration Full Scale

Fig. 2

Root End View of Test Blades

Fig. 3

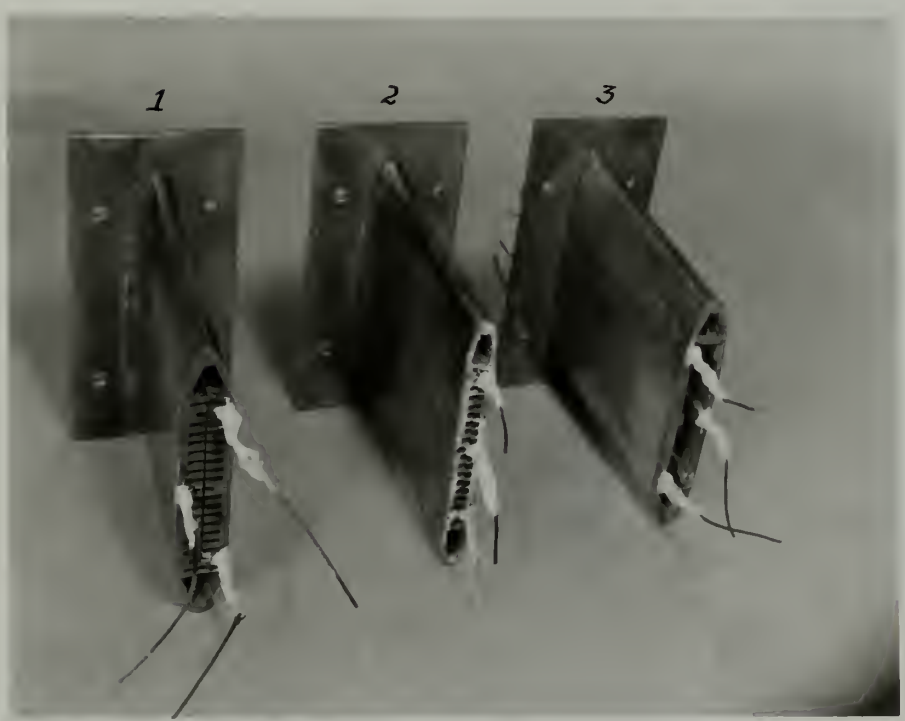

Tip End View of Test Blades

Fig. 4

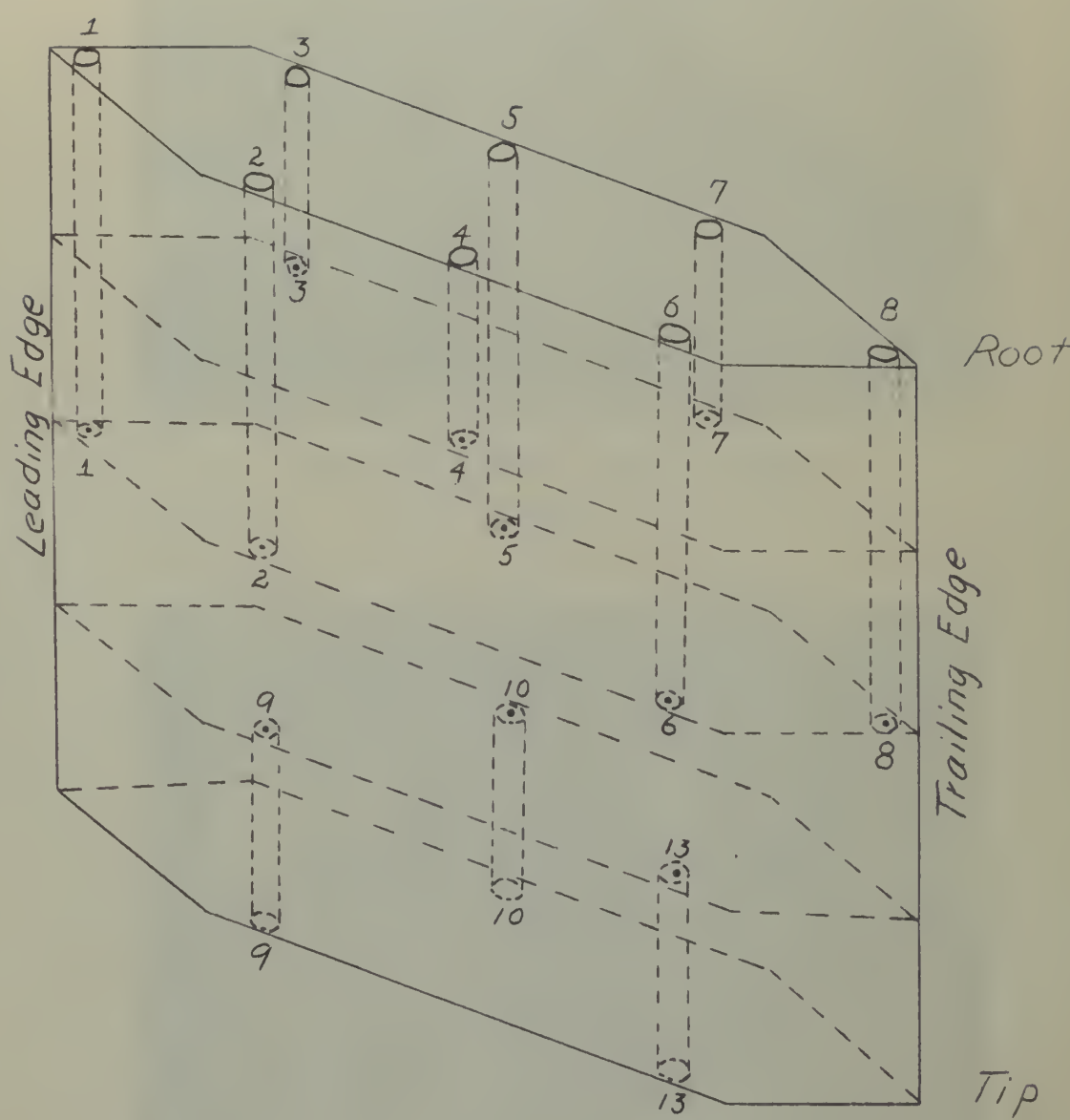

Schematic Orthoganal View of Test Blades
Showing Method of Locating Thermocouples

Fig. 5

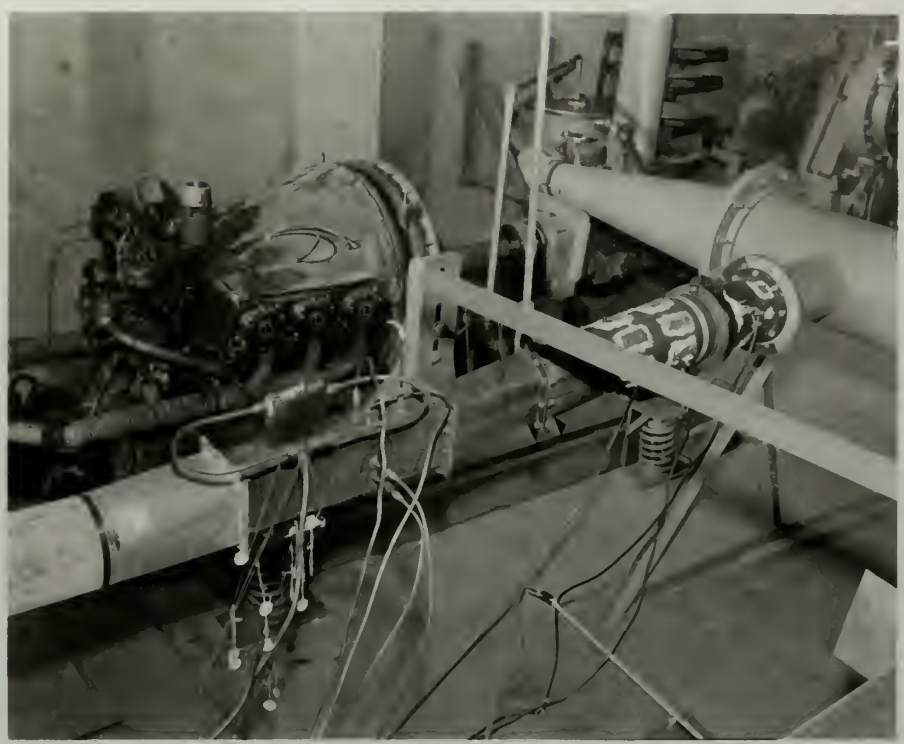

Test Section and Set Up

Fig. 6

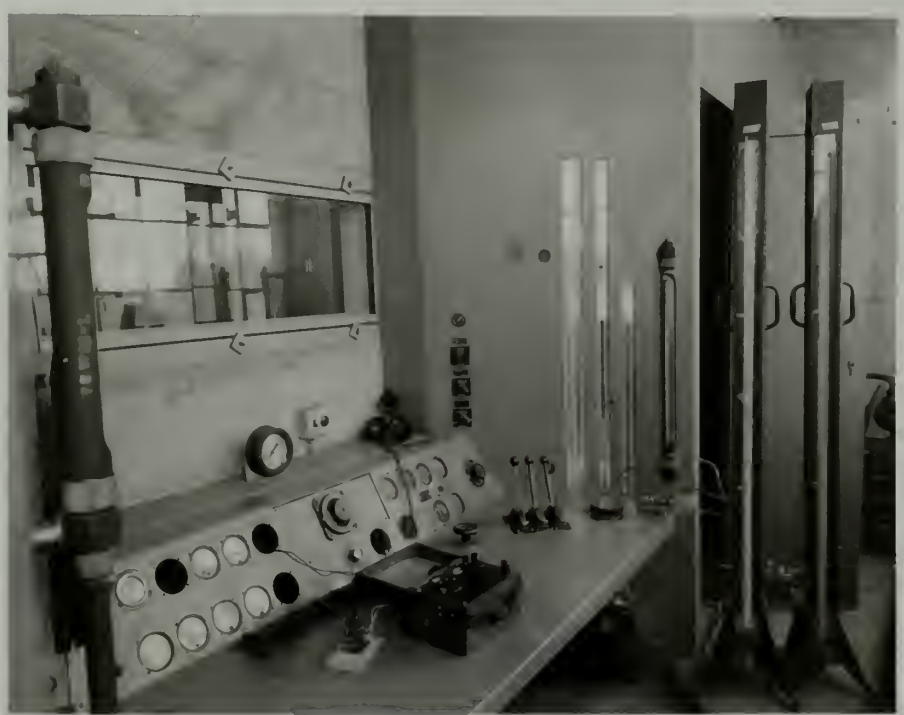

Control Panel

Fig. 7

Spanwise and Chordwise Blade Temperatures at Various Cooling Air Flow Rates

Blade 1 Fin

Gas Temp 800°F

Total Wetted Area Inside Blade .838 ft²

Blade Temperatures (°F)

800
700
600
500

Uncorrected Cooling Air Flow Rates (CFM)

		Corrected
○	0	
△	4	4.88
□	6	8.82
▽	8	13.04

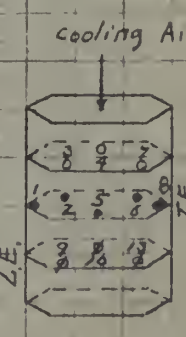

3 4 7 1 2 5 6 8 9 10 13

Chordwise Thermocouple Locations at ¼, ½, ¾ Blade Span

○ ● ◑

Spanwise and Chordwise Blade Temperatures at Various Cooling Air Flow Rates

Blade 2 Fin

Gas Temp. 800°F

Total Wetted Area Inside Blade .656 ft²

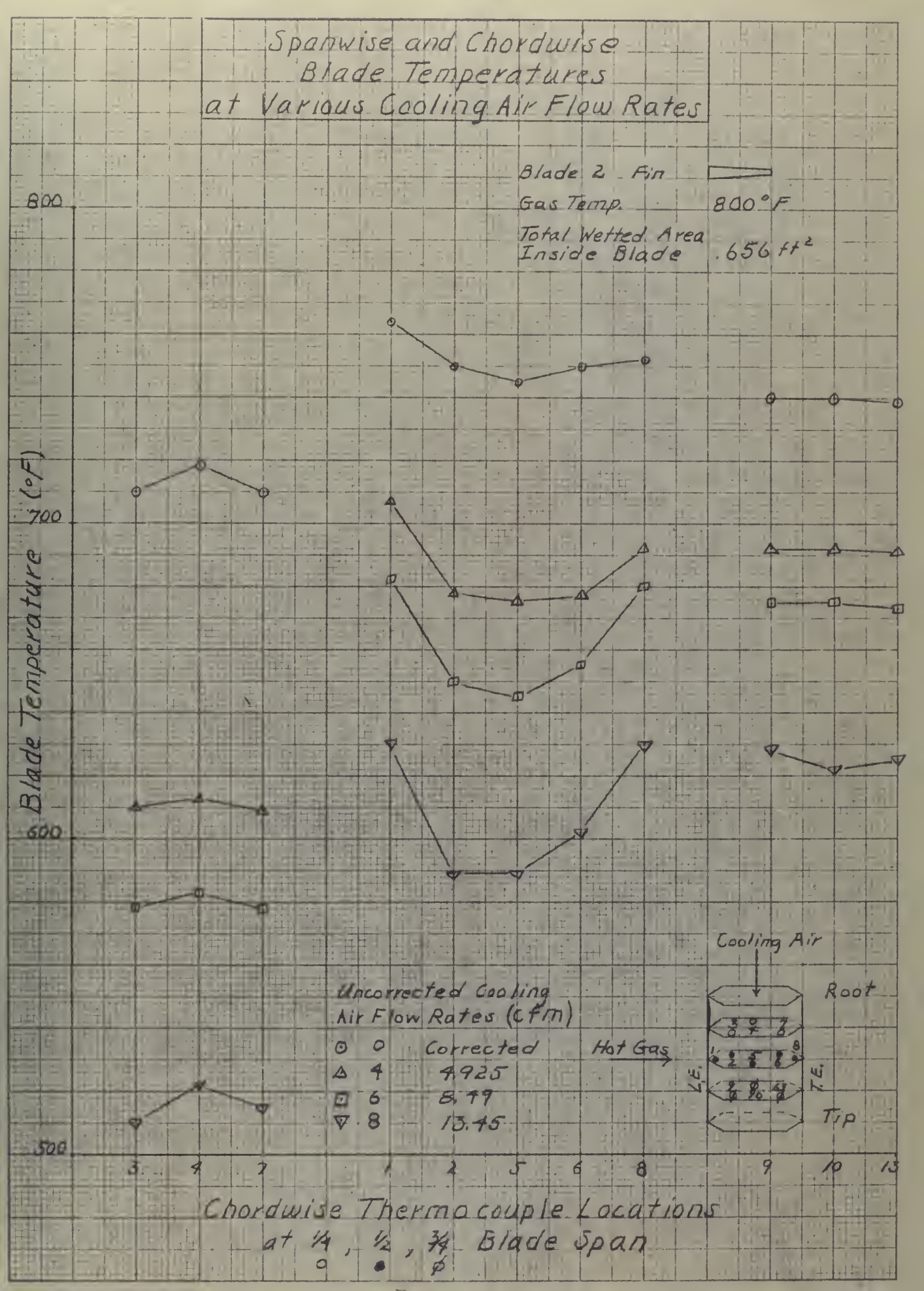

Spanwise and Chordwise Blade Temperatures at Various Cooling Air Flow Rates

Blade 3 Fin

Gas Temp 800° F

Total Wetted Area Inside Blade .5932 ft²

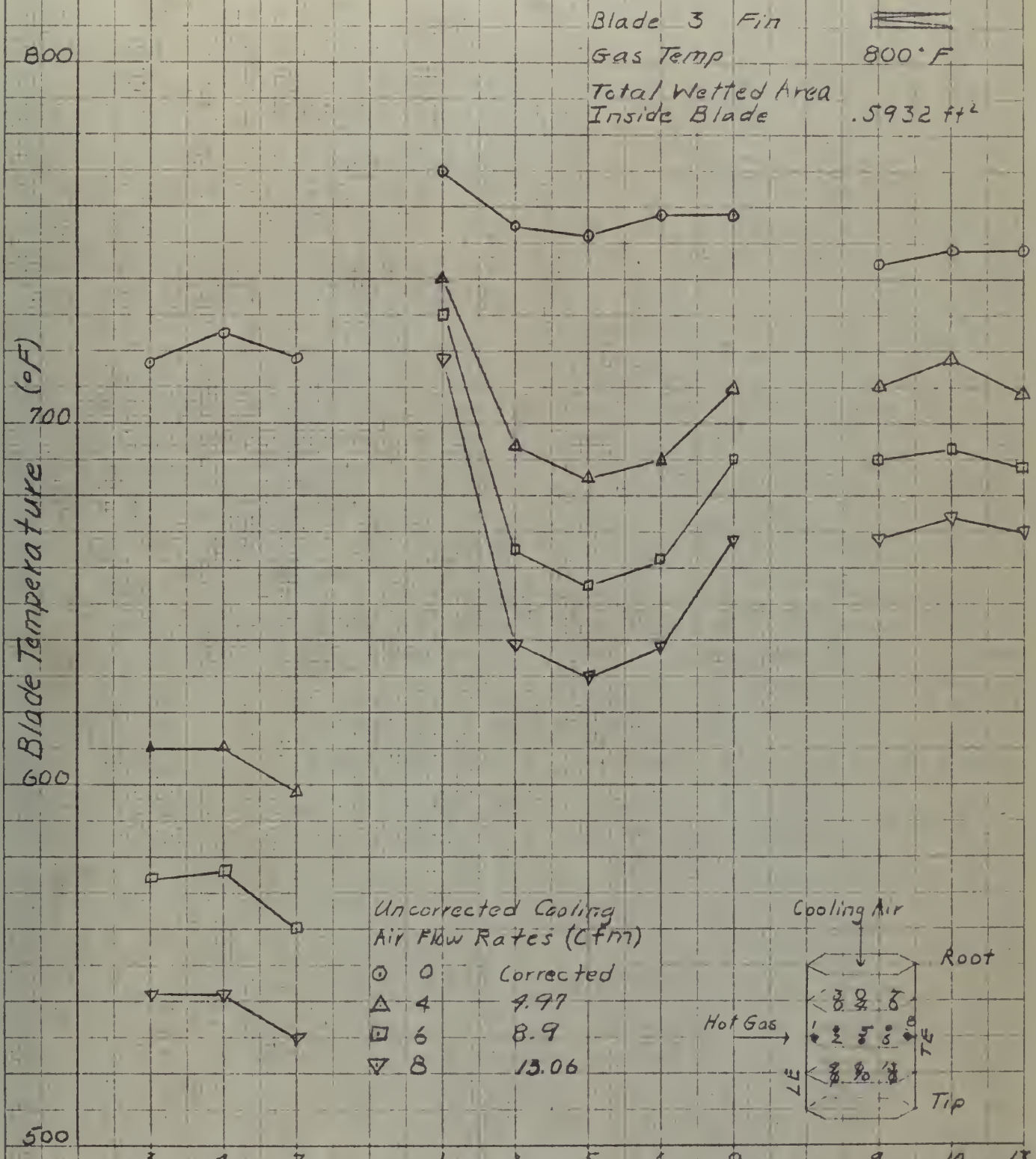

Uncorrected Cooling Air Flow Rates (Cfm)

⊙	0	Corrected
△	4	4.97
⊡	6	8.9
▽	8	13.06

Spanwise and Chordwise Blade Temperatures at Various Cooling Air Flow Rates

Blade 1 Fin
Gas Temp 1100°F
Total Wetted Area Inside Blade .838 ft²

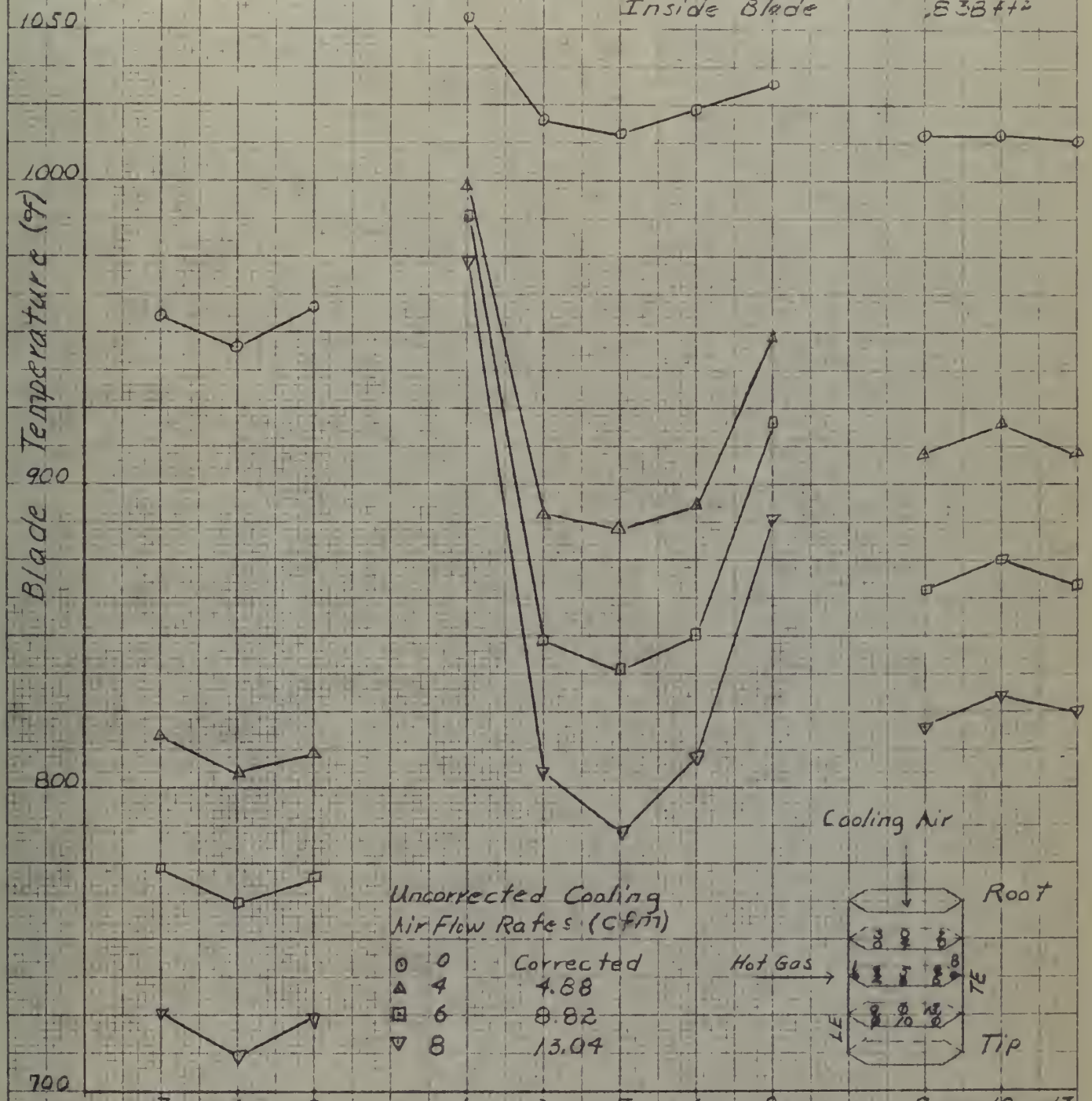

Uncorrected Cooling Air Flow Rates (CFM)

		Corrected
⊙	0	
△	4	4.88
□	6	8.82
▽	8	13.04

Chordwise Thermocouple Locations at ¼, ½, ¾ Blade Span
○ ● ∅

Spanwise and Chordwise Blade Temperatures at Various Cooling Air Flow Rates

Blade 2

Gas Temp 1100°R

Total Wetted Area Inside Blade .656 ft²

Blade Temperature (°F)

1050
1000
900
800
700
650

Uncorrected Cooling Air Flow Rates (Cfm)

⊙	0	Corrected
△	4	4.925
⊡	6	3.49
▽	8	15.45

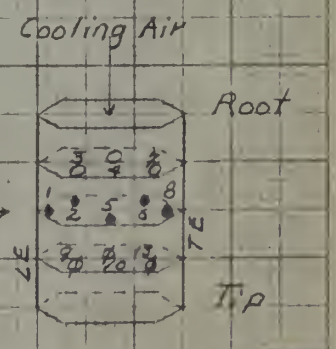

3 4 7 1 2 5 6 8 9 10 11

Chordwise Thermocouple Locations at 1/4, 1/2, 3/4 Blade Span

○ ● ∅

Spanwise and Chordwise Blade Temperatures at Various Cooling Air Flow Rates

Blade 3 Fin

Gas Temp. 1100°F

Total Wetted Area Inside Blade .5932 ft²

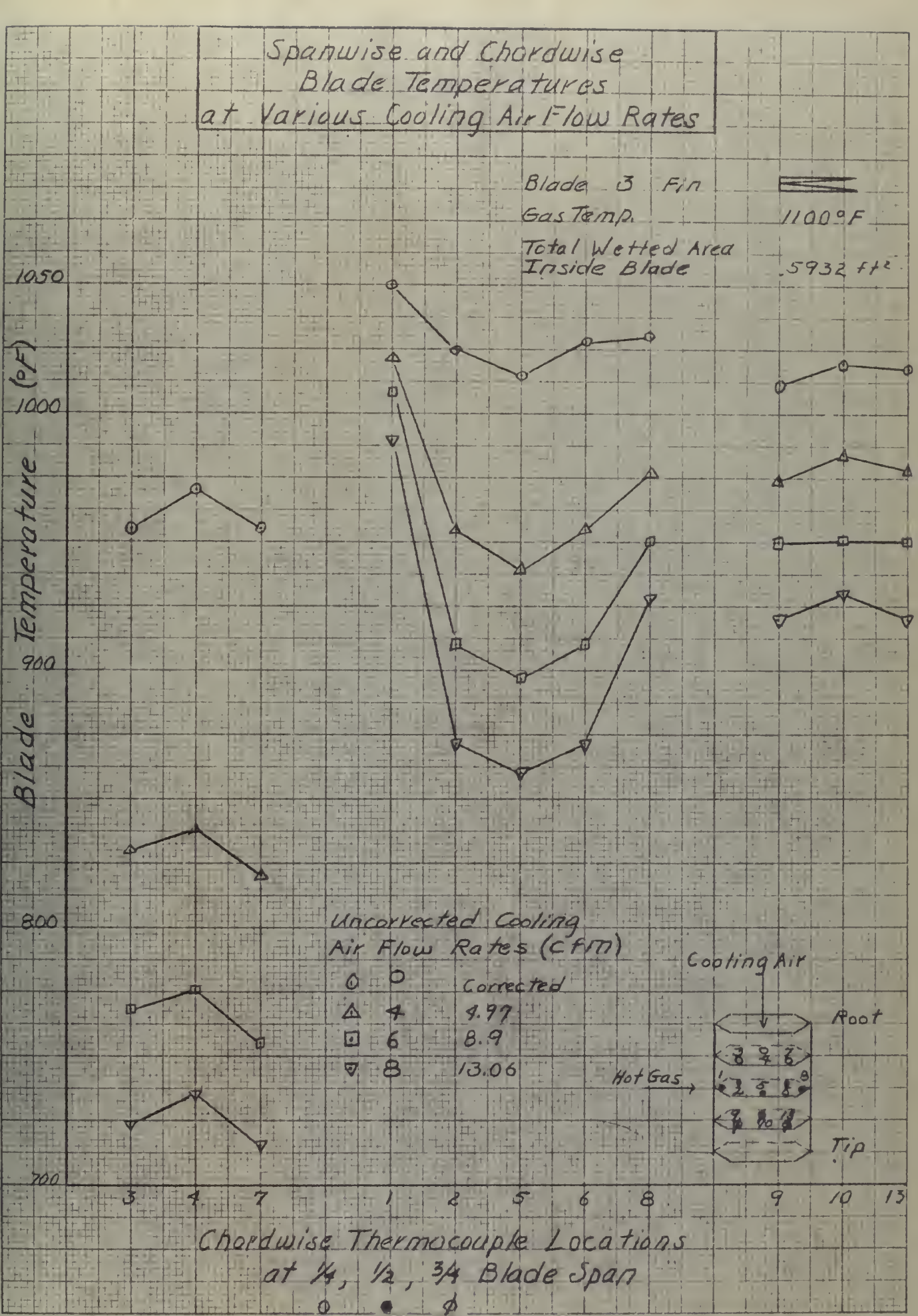

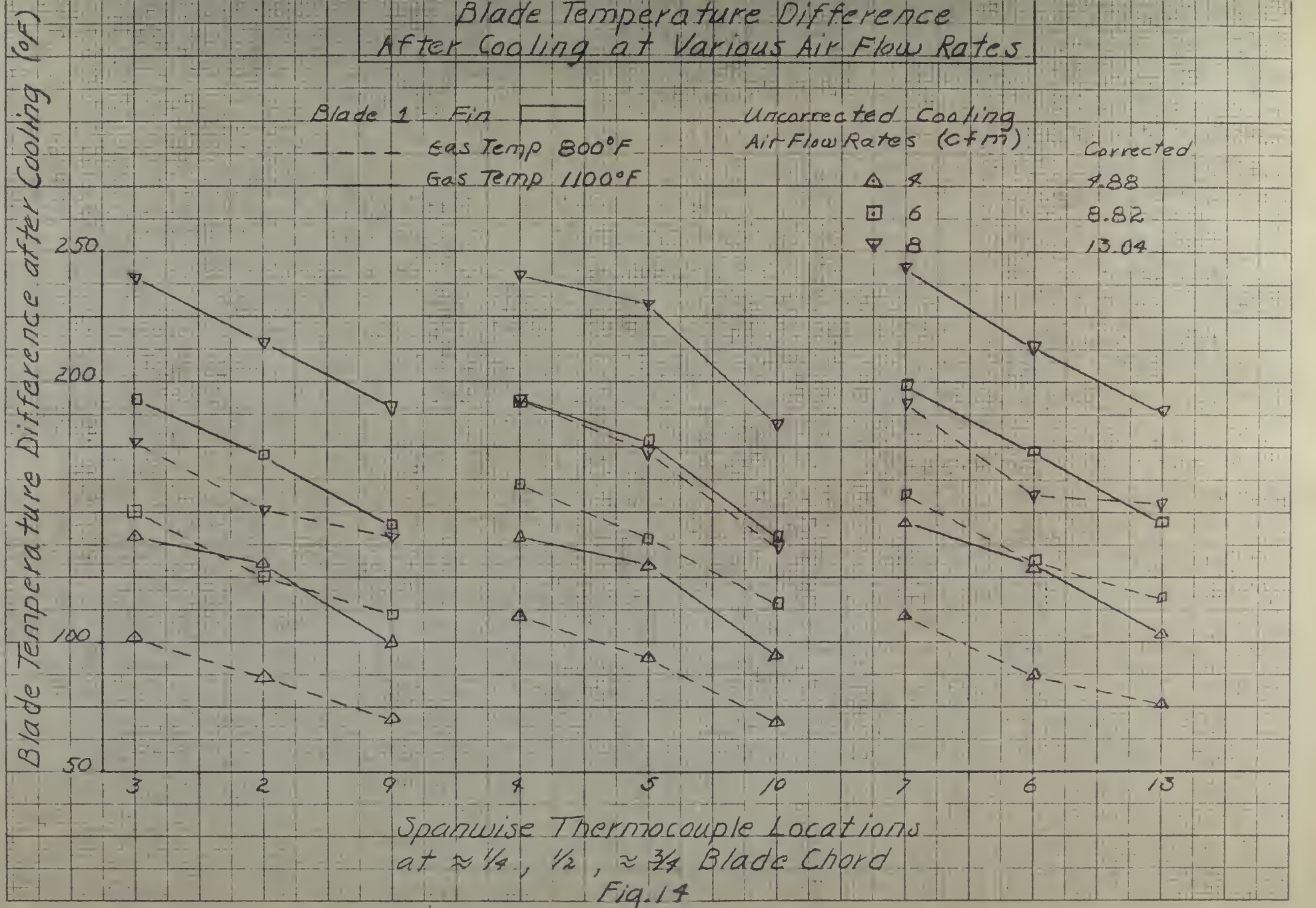
Blade Temperature Difference
After Cooling at Various Air Flow Rates
Blade 1 Fin
Gas Temp 800°F
Gas Temp 1100°F
Uncorrected Cooling
Air-Flow Rates (cfm)
Corrected
4 4.88
6 8.82
8 13.04
Blade Temperature Difference after Cooling (°F)
250
200
100
50
3 2 9 4 5 10 7 6 13
Spanwise Thermocouple Locations
at ≈ 1/4, 1/2, ≈ 3/4 Blade Chord

Fig. 14

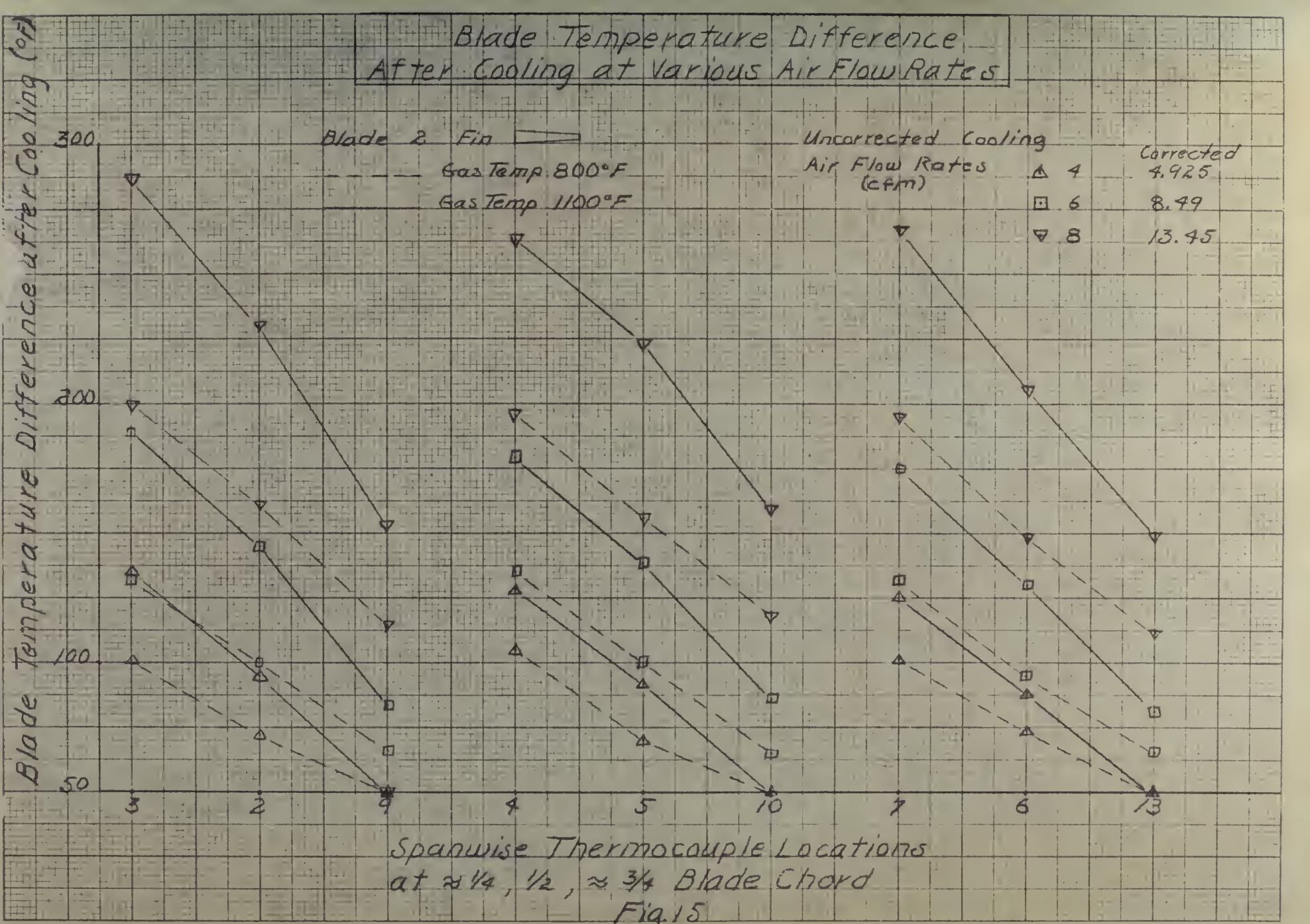
Blade Temperature Difference After Cooling at Various Air Flow Rates
Blade 2 Fin
Gas Temp 800°F
Gas Temp 1100°F
Uncorrected Cooling Air Flow Rates (cfm)
4
6
8
Corrected
4.925
8.49
13.45
Blade Temperature Difference after Cooling (°F)
300
200
100
50
3
2
9
4
5
10
1
6
13
Spanwise Thermocouple Locations at ≈ 1/4, 1/2, ≈ 3/4 Blade Chord

Fig. 15

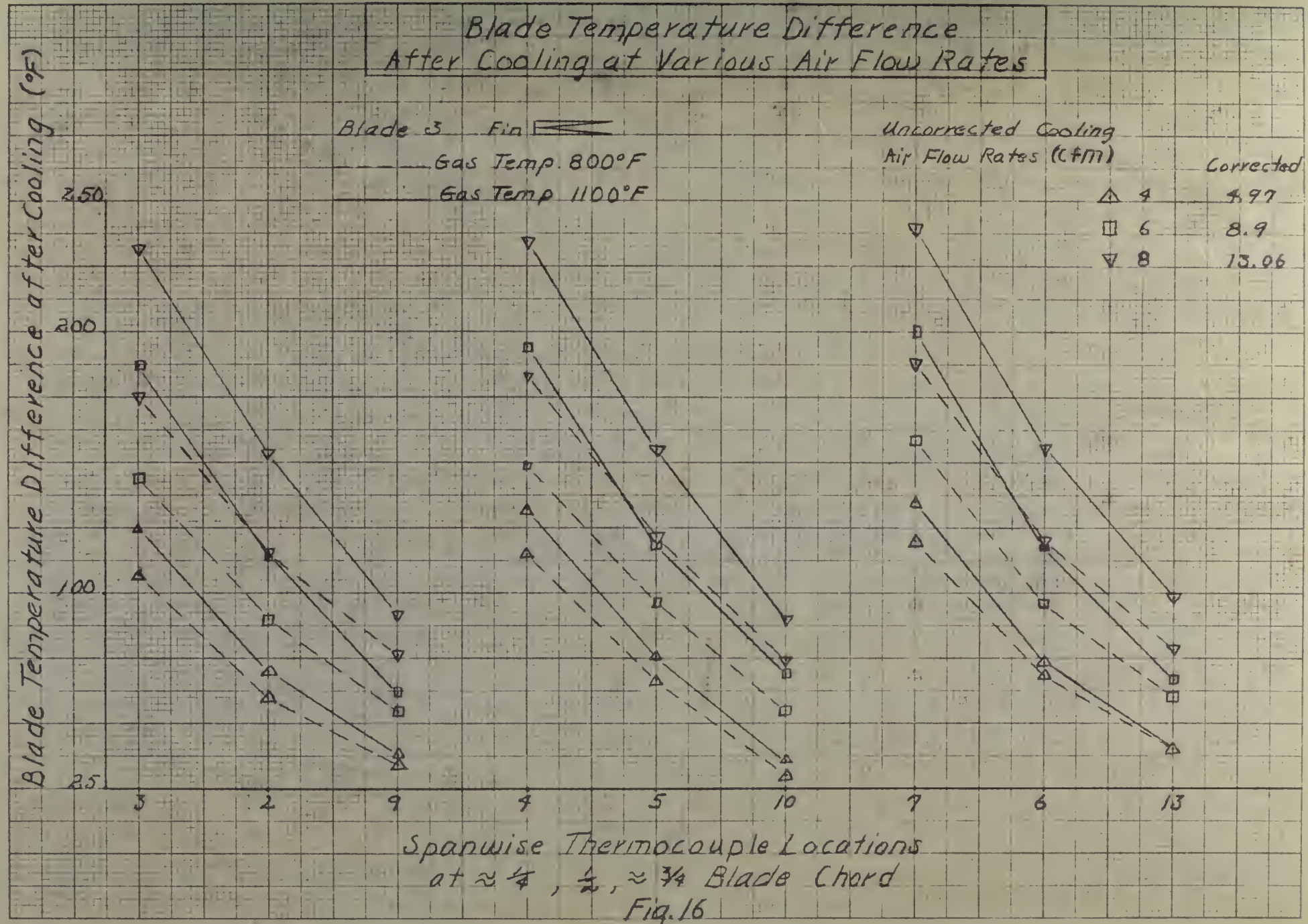
Blade Temperature Difference
After Cooling at Various Air Flow Rates
Blade 3 Fin
Gas Temp. 800°F
Gas Temp 1100°F
Uncorrected Cooling
Air Flow Rates (cfm)
Corrected
4
4.97
6
8.9
8
13.06
Blade Temperature Difference after Cooling (°F)
250
200
100
25
3
2
9
4
5
10
7
6
13
Spanwise Thermocouple Locations
at ≈ ¼ , ½ , ≈ ¾ Blade Chord

Fig. 16

Ratio of Blade Temperature Reduction To Gas Temperature

Blade 1 Fin

$$\phi = \frac{\text{Blade Temperature Reduction}}{\text{Gas Temp.} - \text{Cooling Air Entrance Temp.}}$$

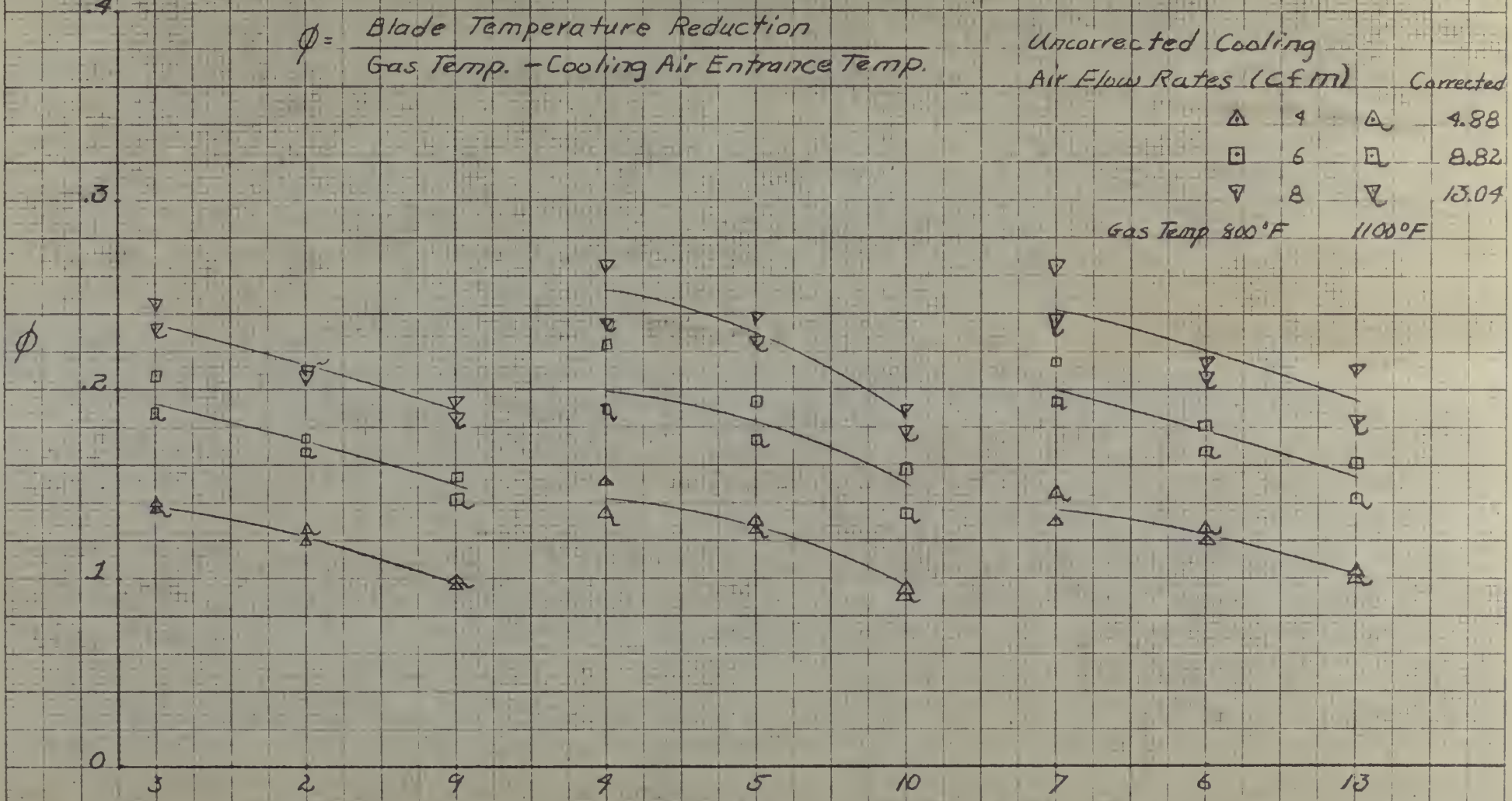

Spanwise Thermocouple Locations at ≈¼, ½, ≈¾ Blade Chord

Fig. 17

Ratio of Blade Temperature Reduction To Gas Temperature

Blade 2 Fin

$$\phi = \frac{\text{Blade Temperature Reduction}}{\text{Gas Temp} - \text{Cooling Air Entrance Temp.}}$$

Uncorrected Cooling Air Flow Rates (cfm)			Corrected
△	4	△	4.925
□	6	□	8.49
▽	8	▽	13.45

Gas Temp. 800°F. 1100°F.

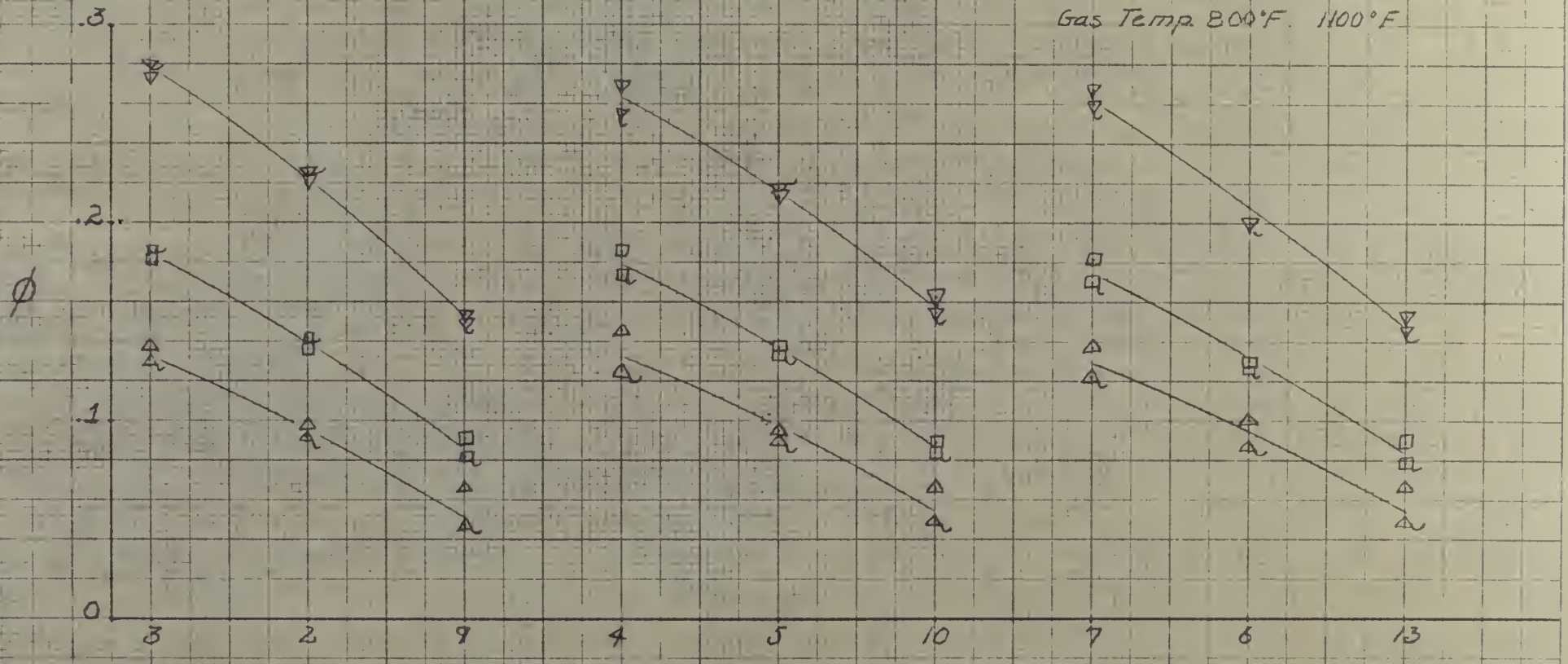

Spanwise Thermocouple Locations at ≈ ¼, ½, ≈ ¾ Blade Chord

Fig. 18

Ratio of Blade Temperature Reduction To Gas Temperature

Blade 3 Fin

$$\phi = \frac{\text{Blade Temperature Reduction}}{\text{Gas Temp.} - \text{Cooling Air Entrance Temp.}}$$

Uncorrected Cooling Air Flow Rates (Cfm)			Corrected
△	4	△	4.97
□	6	□	8.9
▽	8	▽	13.06

Gas Temp. 800°F 1100°F

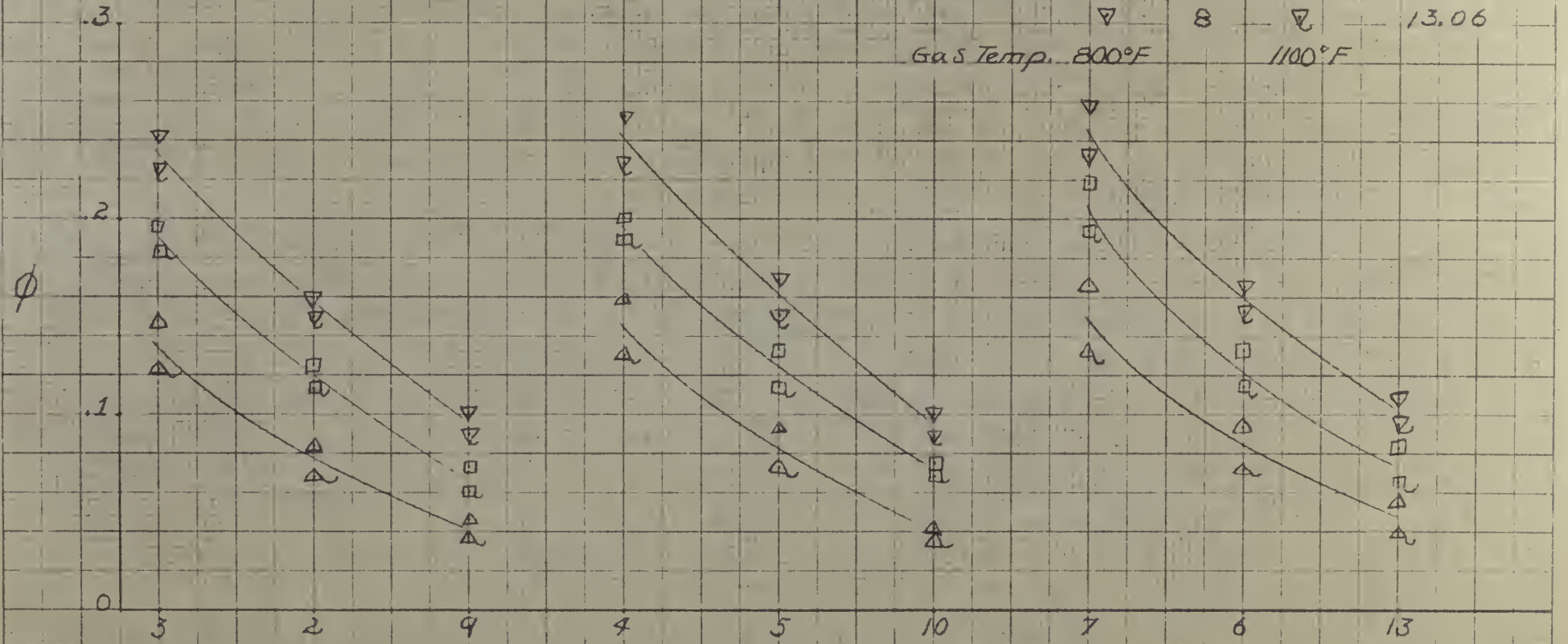

Spanwise Thermocouple Locations at ≈ 1/4, 1/2, ≈ 3/4 Blade Chord

Fig. 19

Ratio of Inside Film Heat Transfer Coefficient To Outside Film Heat Transfer Coefficient For Three Test Blades

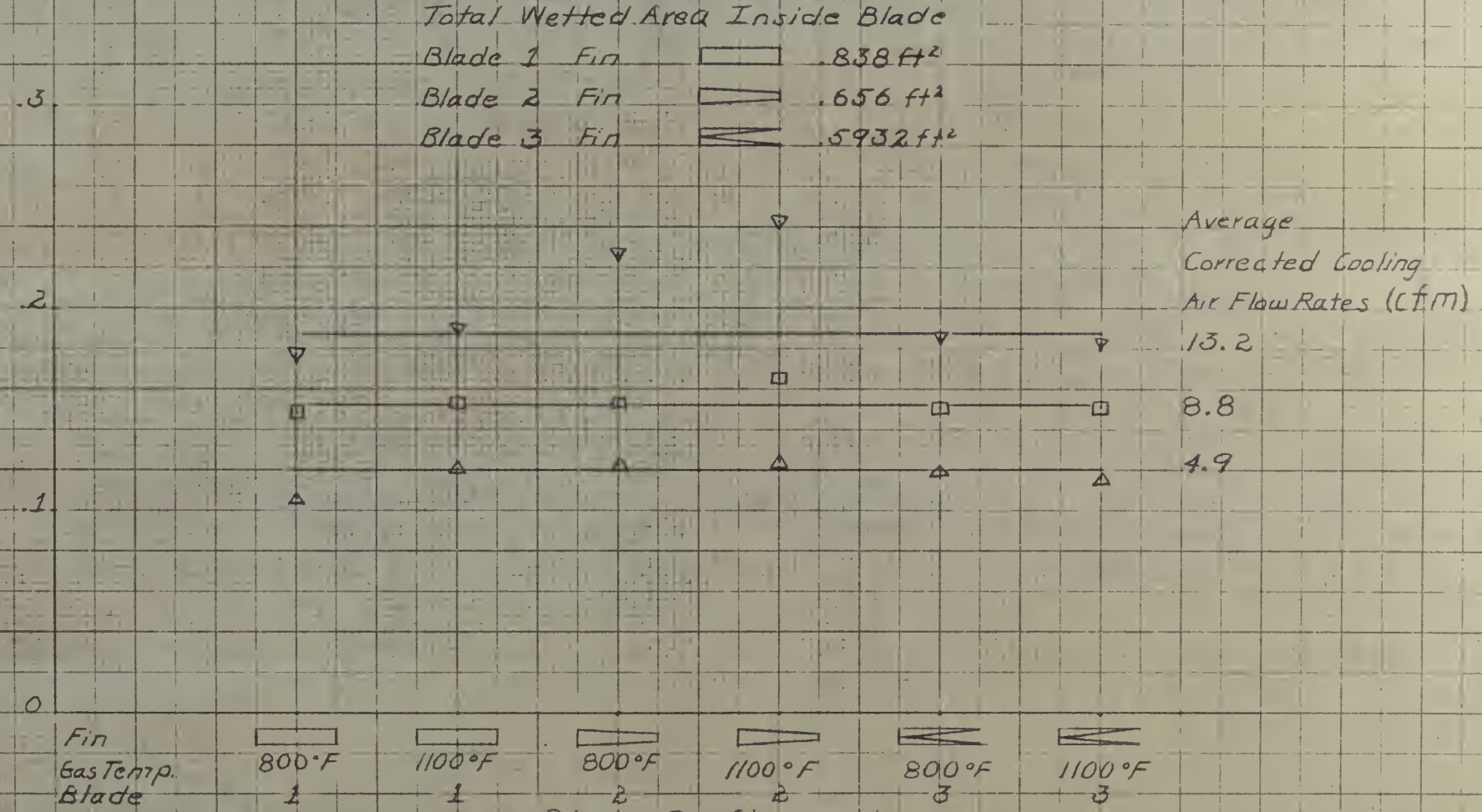

Blade Configuration

Fig. 20

Ratio of Inside to Outside Film Heat Transfer Coefficient vs Cooling Air Flow

Applicable For Three Test Blades Used and any Gas Temperature

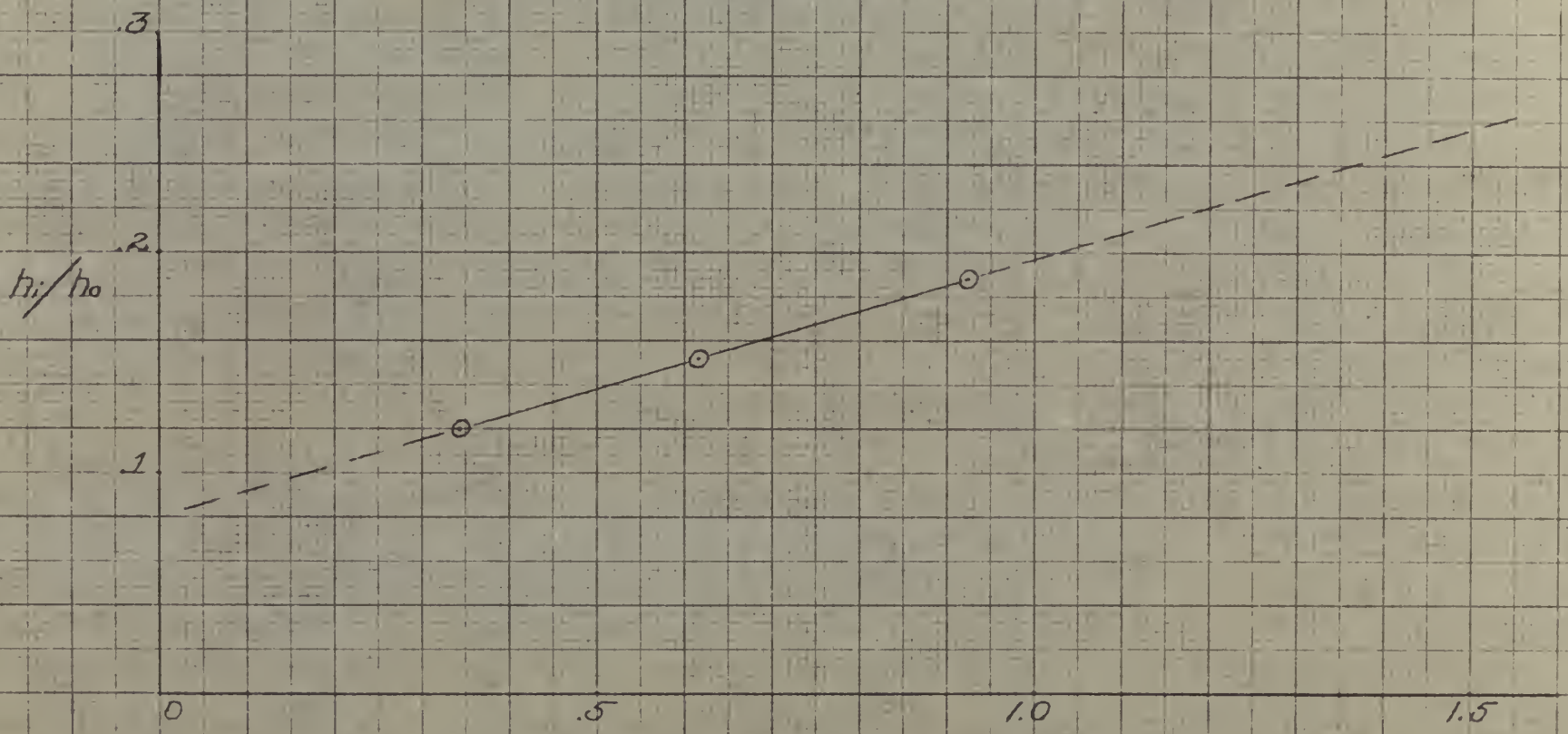

Fig. 21

Sample Calculations

(1.) Estimate of heat loss or addition at total temperature Probe by: (a) Conduction, (b) Radiation.

(a.) Conduction

Assume: Inside gas temperature, $T_g = 1100°F$
Test Section Wall Temperature, $T_w = 910°F$

From Ref 7

$$\theta_2 = \frac{\theta_1}{\cosh m l} \quad , \quad m = \sqrt{\frac{hC}{kA}}$$

Where:

θ_2 = excess temperature at end of rod, °F.
θ_1 = difference between gas and wall temperature, °F.
l = length of rod in feet.
h = film heat transfer coeficient, BTU/hr ft² °F
C = circumference of rod, ft.
A = cross sectional area of rod, ft².
k = thermal conductivity of material, BTU/hr ft² °F/ft.

From Ref. 10

For Turbulent air flow across single rod

$$h = .025 \frac{G^{.58}(1 + .0005t)}{D^{.42}}$$

Where:

G = mass velocity through the minimum free area between the rods, lb/hr ft²
D = outside tube diameter, ft
t = average air temperature, °F

Calculation for hollow steel tube, inside diameter = 1/8"
outside diameter = 5/16"

$\theta_1 = 200°F$
$\theta_2 = 8°F$ (allowable error)
$G = 165{,}500$ lbs/hr ft² using Mach Number in Test Section, $M = .3$
$D = .0156$ ft

$t = 1100°F$

$h = \underline{250}$ BTU/hr ft²°F

$A = .0001065$ ft²

$C = \pi/64$ ft

$k = 17.75$ BTU/hr ft²°F/ft (for steel at 1100°F)

$m = \underline{80.5}$

$\frac{\theta_1}{\theta_2} = \cosh ml = 25$

$ml = 3.91$

$\underline{l = .584"}$

$$h = (.025)\frac{(165{,}500)^{.58}[1+(.000576)(1100)]}{(.0156)^{.42}}$$

$$m = \sqrt{\frac{(250)(\pi)}{(17.75)(64)(.0001065)}}$$

Therefore probe should not be placed closer than .6" from the test section wall to keep within the allowable error of 8°F.

(1.) (b) Radiation

From Ref 9

$$q_2 = \sigma F_e F_A A_1 F_c (T_1^4 - T_2^4) \text{ BTU/hr}$$

Where

q_2 = net heat exchange between two surfaces.

σ = Stefan-Boltzmann constant.

F_e = factor to allow for departure from black body.

F_A = configuration factor

A_1 = area of thermocouple bead, ft².

Radiation exchange between thermocouple bead and walls of test section.

$F_A = 4/3$

$F_e = .284$

$A = \frac{(\pi)(.0016)}{144}$ ft² (bead diameter = .04")

$T_1 = 1560°R$

$T_2 = 1360°R$

$\sigma = .174 \times 10^{-8}$

$q = \underline{.0291}$ BTU/hr (lost)

$$q = (.174\times10^{-8})(.284)\tfrac{4}{3}\frac{(\pi)(.016)}{(144)}\left[(1560)^4-(1360)^4\right]$$

Radiation exchange between thermocouple bead and flame.

From Ref. 9

$$q = \left[\sigma A (T_F^4 - T_W^4) \rho_F \rho_W F_c\right] \text{ BTU/hr}$$

where

ρ_F = emissivity of flame.

ρ_W = emissivity of bead.

F_c = factor to allow for effective area of thermocouple bead.

$F_c = \frac{1}{30}$

$\rho_W = .284$

$\rho_F = .5$

$T_F = 3960°R$

$T_W = 1560°R$

$q = .0394$ BTU/hr (added) $\left[q = (.174)10^{-8} \frac{(\pi)(.0016)}{144}(.284)(.5)\frac{1}{30}\left[(3960)^4 - (1560)^4\right]\right]$

Net heat loss from bead due to radiation.

$(q_2 - q) = hA(\Delta T)$

where

h = film heat transfer coefficient calculated for air flow across a rod.

$(q_2 - q) = +.0103$ BTU/hr

$h = 250$ BTU/hr ft^2 °F

$A = \frac{\pi(.0016)}{144}$ ft^2

$\Delta T = 1.18°F$ (added) $\left[\Delta T = \frac{(.0103)(144)}{(250)\pi(.0016)} \text{ °F}\right]$

(2.) Estimation of probable error.

From Ref. 12 and 4

$$R = \sqrt{r_1^2 + r_2^2 + \cdots + r_n^2}$$

where

R = probable error

r = individual errors.

For Leeds and Northrup Potentiometer Indicator used

error = .3% of range = (.003)(2000) = ±6°R F

$r_1 = \pm 6°R F$

Personal error in reading temperatures and manipulating controls = ±5°F

$r_2 = \pm 5°F$

$\underline{R = \pm 8°F}$ $\quad R = \sqrt{(6)^2+(5)^2}$

(3.) Reynold's Number calculation for flow of cooling air inside blades. Calculation for Blade 1 at highest rate of cooling gas flow, gas temperature = 800°F.

$$\frac{\rho V d_w}{\mu} = R_e$$

Sutherland's Formula

$$\mu = (.371 \times 10^{-6})\left[\frac{(734.4)}{T+216}\left(\frac{T}{518.4}\right)^{3/2}\right]$$

where

ρ = density of air, lbs sec²/ft⁴.

V = velocity, ft/sec.

μ = viscosity, lbs sec/ft²

d_w = hydraulic diameter (applicable for fully developed flow).

T = absolute temperature °R.

T = 621.5°R (average cooling air temp)

$\mu = (.427)(10^{-6})$ lbsec/ft² $\quad \left[\mu = (.371 \times 10^{-6})\left[\frac{734.4}{621.5+216}\left(\frac{621.5}{518.4}\right)^{3/2}\right]\right]$

$\rho = .0022$ lbs sec²/ft⁴ (100°F and 14.7 psia)

$$V = \frac{w}{\rho A} = \frac{(.0156)}{(.071)(.00802.5)} = 27.4 \text{ ft/sec}$$

$$d_w = \frac{4(\text{cross sectional area})}{\text{perimeter}} = \frac{(4)(.005025)}{2.01} = .01598 \text{ ft}$$

$\underline{R_e = 2255}$ $\quad \left[r_e = \frac{(.0022)(27.4)(.01598)}{(.427)(10^{-6})}\right]$

(4.) Determination of inside film heat transfer coefficient, h_i, for use in determining blade wall temperature difference and fin effectiveness.

From Ref. 7

$Nu = \frac{h_i b}{k} = 3.75$ (For fully developed flow in passage)

Where

Nu = Nusselt's Number

k = thermal conductivity of air = .0166 BTU/hr ft °F/ft

b = fin spacing, ft = .1/12 ft

h_i = 7.48 BTU/hr ft² °F $\left[h_i = \frac{(3.75)(.0166)(12)}{.1} \right]$

⑤ Determination of outside film heat transfer coefficient, h_o, for use in determining blade wall temperature difference.

From Ref. 9

$h_o = \frac{V^{3/4}}{830 L^{1/4}}$ (For flow of gases parallel to plane surfaces.)

Where

V = velocity in ft/hr = (727)(3600) ft/hr

L = length of blade in ft = 4.3/12 = .358 ft

Calculation for gas temperature = 1100°F

Mach Number of blade, $M = .382$

h_o = 102.2 BTU/hr ft² °F $\left[h_o = \frac{[(727)(3600)]^{3/4}}{(830)(.358)^{1/4}} \right]$

⑥ Determination of temperature difference across blade wall.

From Ref. 7

$U = \frac{1}{\frac{1}{h_i} + \frac{x}{k} + \frac{1}{h_o}}$ = over all coefficient of transmission

Where

x = blade width (skin) ft = .0164 ft

k = thermal conductivity of material

k (for mild steel at 850°F) = 22.1 BTU/hr ft² °F/ft

h_i and h_o same as for calculation ④ and ⑤.

Calculation for gas temperature = 1100°F

$U = 6.99$ BTU/hr ft² °F

$$U = (t_1 - t_4) = \frac{k}{x}(t_2 - t_3) \qquad \left[U = \frac{1}{\frac{1}{7.98} + \frac{.0164}{22.1} + \frac{1}{102.2}} \right]$$

$t_4 \approx 200°F$

$t_1 = 1100°F$

$(t_2 - t_3) = 3.66°F = \Delta T$ $\qquad \left[\Delta T = \frac{(6.99)(900)(.0164)}{22.1} \right]$

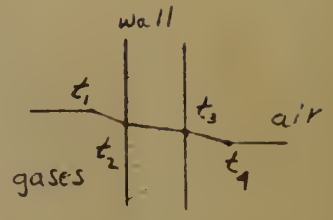

(7) Determination of fin effectiveness, η_f, Blade 1.

Gas temperature = 1100°F

From Ref. 8

$$\eta_f = \frac{\tanh n}{n}$$

where

$$n = L\sqrt{\frac{h}{k y_0}}$$

L = fin height ft = .225/12 = .01875 ft

h = same as for calculation (4) = 7.98 BTU/hr ft² °F

k = thermal conductivity of material

Same as for calculation (6) = 22.1 BTU/hr ft² °F/ft

y_0 = semi fin width, ft = .05/2(12) = .00208 ft

$n = .239$ $\qquad \left[n = .01875\sqrt{\frac{7.98}{(22.1)(.00208)}} \right]$

$\tanh n = .235$

$\eta_f = .984$ $\qquad \left[\eta_f = \frac{.235}{.239} \right]$

(8) Determination of ratio of inside to outside film heat transfer coefficient, h_i/h_o, from experimental data.

From Ref. 7

$Q_o = h_o A_o (T_g - T_{wo})$ $\quad Q_o = Q_i$

$Q_i = h_i A_i (T_{wi} - T_a)$

$$h_i/h_o = \frac{A_o}{A_i} \frac{(T_g - T_{wo})}{(T_{wi} - T_a)\eta_f}$$

Where

A_o = total outside wetted perimeter of blade, ft.

A_i = total inside wetted perimeter of blade, ft.

T_g = Gas temperature

T_a = Cooling Air temperature, average.

T_w = Measured blade wall temperature, average.

T_{wi} = Inside Wall Temperature, $= T_w - \frac{1}{2}\Delta T$.

T_{wo} = Outside Wall temperature, $= T_w + \frac{1}{2}\Delta T$.

Calculation is for Blade 1, gas temperature = 1100°F, highest rate of cooling air flow used, middle thermocouple level.

$A_o = .744$ ft $\quad T_w = 800°F$

$A_i = 2.01$ ft $\quad T_{wo} = 801.83°F$

$T_g = 1100°F$ $\quad T_{wi} = 798.17°F$

$T_a = 206.5°F$ $\quad \eta_f = .984$

$h_i/h_o = .1895$

$$\left[h_i/h_o = \frac{(.744)}{(2.01)} \frac{1}{(.984)} \frac{(1100 - 801.83)}{(798.17 - 206.5)} \right]$$

(9) Weight Flow of Cooling Air Calculations.

Flow rater equation from instrument handbook.

$$Q_1 = Q_A \left(\frac{p_a}{p_2}\right)^{1/2} \left(\frac{T_2}{T_A}\right)^{1/2} \qquad W_A = \rho Q_1$$

where

Q_A = cooling flow rate, meter reading, cfm.

Q_1 = corrected flow rate of cooling air.

p_2 = 14.7 psia (meter calibration)

p_a = cooling air pressure absolute.

T_2 = 560°R (meter calibration)

T_A = Cooling Air inlet temperature °R.

W_a = Weight flow of cooling air at 100°F and 14.7 psia

ρ = density of air = .071 lbs/cuft at 100°F and 14.7 psia

$$W_a = (\rho)(Q_A)\left(\frac{560}{14.7}\right)^{1/2}\left(\frac{P_a}{T_A}\right)^{1/2} \text{ lbs/min}$$

Calculation for Blade 1 at gas temperature 800°F

$T_A = 536°R$

$P_a = 21.08$ psia

$Q_A = 4$ cfm

$Q_1 = 4.88$ cfm

$W_a = .3473$ lbs/min $\quad \left[W_a = (.938)(4)\left(\frac{21.08}{536}\right)^{1/2}\right]$

(10) Burner air flow calculations.

From Ref. 6

$$w = .668\, A_2 K E \sqrt{\rho_1 \Delta p} \text{ lbs/sec}$$

or $$w = 2.52\sqrt{\frac{p h_w}{T}} \text{ lbs/sec}$$

Where

A_2 = cross sectional area of orifice = 24.62 in^2

w = weight flow of burner air, lbs/sec.

ρ_1 = density of air, lbs/ft^3.

Δp = pressure drop across orifice, lbs/in^2.

$K = .7$ = flow coefficient

$E = 1$ = area multiplier for thermal expansion of primary element.

p = barometric pressure (inches of mercury)

h_w = pressure drop across orifice (inches of water)

T = burner air inlet temperature °R.

Calculation for gas temperature = 800°F, Blade 1.

$p = 29.22$ inches of mercury

$h_w = 19.5$ inches of water

$T = 508°R$

$w = 2.67$ lbs/sec $\quad \left[w = 2.52\sqrt{\frac{(29.22)(19.5)}{508}}\right]$

(11) Mach Number Calculation

using Isentropic relationship

$$\frac{P_s}{P_o} = \left(1 + \frac{\gamma-1}{2} M^2\right)^{\frac{\gamma-1}{\gamma}}$$

The mach number, M, was obtained from NACA TN 1592 in which M is tabulated against pressure ratio at standard atmospheric conditions.

P_s = test section static pressure.

P_o = test section total pressure.

The value thus obtained was then corrected to account for the change in temperature and γ.

Calculation is for blade 1 at gas temperature = 600°F

P_s (average) = 28.95 inches of mercury absolute.

P_o = 32.92 inches of mercury absolute.

M = .458 from tables.

$M = \frac{V}{a} = \frac{V}{\sqrt{\gamma RT}}$, therefore correction factor $= \sqrt{\frac{(520)(1.4)}{(1260)(1.353)}}$

$= .653$

Corrected test section $M = (.653)(.458) = \underline{\underline{.3}}$

Calculation for M at blades, using NACA TN 1592.

for Me .3, $A^*/A = .4919$

A_1 = cross sectional area of test section = 15.75 in²

$A^* = .4919/15.75 = 7.74$ in²

A_2 = cross sectional area of test section at blade = 12.6 in²

$A^*/A_2 = .613$

$M = \underline{\underline{.382}}$ for $A^*/A_2 = .613$ (from tables)

(12.) Determination of dynamic temperature increase at leading edge of blade over the wall of blade.

From Ref 7

$$\theta = \frac{V^2}{12000}(1-\sigma)$$

Where

θ = temperature increase in °F.

V = velocity of gases in ft/sec.

σ = recovery factor (for flow along a cylinder)

Calculation for gas temperature = 800°F, Blade 1.

$M = .382$

$V = 652$ ft/sec

$\sigma = .84$

$\underline{\underline{\Theta = 5.67°F}}$

$$\left[\Theta = \frac{(652)^2}{12000}(1-.84)\right]$$

Thesis
L26 Laney 17332

Thermal effects in air cooled
turbine blades.